



## International Geology Review

Publication details, including instructions for authors and subscription information:

<http://www.tandfonline.com/loi/tigr20>

### Magmatic garnet in the Triassic (215 Ma) Dehnow pluton of NE Iran and its petrogenetic significance

Ramin Samadi<sup>a</sup>, Hassan Mirnejad<sup>b</sup>, Hiroshi Kawabata<sup>c</sup>, Chris Harris<sup>d</sup>, Mohammad Vali Valizadeh<sup>b</sup> & Esteban Gazel<sup>e</sup>

<sup>a</sup> Department of Geology, College of Basic Sciences, Tehran Science and Research Branch, Islamic Azad University, Tehran, Iran

<sup>b</sup> Department of Geology, Faculty of Science, University of Tehran, Tehran, Iran

<sup>c</sup> Research and Education Faculty, Kochi University, Kochi, Japan

<sup>d</sup> Department of Geological Sciences, University of Cape Town, Rondebosch, South Africa

<sup>e</sup> Department of Geosciences, Virginia Tech, Blacksburg, VA, USA

Published online: 05 Feb 2014.

To cite this article: Ramin Samadi, Hassan Mirnejad, Hiroshi Kawabata, Chris Harris, Mohammad Vali Valizadeh & Esteban Gazel (2014) Magmatic garnet in the Triassic (215 Ma) Dehnow pluton of NE Iran and its petrogenetic significance, International Geology Review, 56:5, 596-621, DOI: [10.1080/00206814.2014.880659](https://doi.org/10.1080/00206814.2014.880659)

To link to this article: <http://dx.doi.org/10.1080/00206814.2014.880659>

PLEASE SCROLL DOWN FOR ARTICLE

Taylor & Francis makes every effort to ensure the accuracy of all the information (the "Content") contained in the publications on our platform. However, Taylor & Francis, our agents, and our licensors make no representations or warranties whatsoever as to the accuracy, completeness, or suitability for any purpose of the Content. Any opinions and views expressed in this publication are the opinions and views of the authors, and are not the views of or endorsed by Taylor & Francis. The accuracy of the Content should not be relied upon and should be independently verified with primary sources of information. Taylor and Francis shall not be liable for any losses, actions, claims, proceedings, demands, costs, expenses, damages, and other liabilities whatsoever or howsoever caused arising directly or indirectly in connection with, in relation to or arising out of the use of the Content.

This article may be used for research, teaching, and private study purposes. Any substantial or systematic reproduction, redistribution, reselling, loan, sub-licensing, systematic supply, or distribution in any form to anyone is expressly forbidden. Terms & Conditions of access and use can be found at <http://www.tandfonline.com/page/terms-and-conditions>

## Magmatic garnet in the Triassic (215 Ma) Dehnow pluton of NE Iran and its petrogenetic significance

Ramin Samadi<sup>a\*</sup>, Hassan Mirnejad<sup>b</sup>, Hiroshi Kawabata<sup>c</sup>, Chris Harris<sup>d</sup>, Mohammad Vali Valizadeh<sup>b</sup> and Esteban Gazel<sup>e</sup>

<sup>a</sup>Department of Geology, College of Basic Sciences, Tehran Science and Research Branch, Islamic Azad University, Tehran, Iran;

<sup>b</sup>Department of Geology, Faculty of Science, University of Tehran, Tehran, Iran; <sup>c</sup>Research and Education Faculty, Kochi University, Kochi, Japan; <sup>d</sup>Department of Geological Sciences, University of Cape Town, Rondebosch, South Africa; <sup>e</sup>Department of Geosciences, Virginia Tech, Blacksburg, VA, USA

(Received 28 October 2013; accepted 3 January 2014)

The Triassic Dehnow pluton of NE Iran is a garnet-bearing I-type calc-alkaline metaluminous diorite-tonalite-granodiorite intrusion. The parental magma formed as the result of partial melting of intermediate to felsic rocks in the lower crust. Petrological and geochemical evidence, which indicates a magmatic origin for the garnet, includes: large size (~10–20 mm) of crystals, absence of reaction rims, a distinct composition from garnet in adjacent metapelitic rocks, and similarity in the composition of mineral inclusions (biotite, hornblende) in the garnet and in the matrix. Absence of garnet-bearing enclaves in the pluton and lack of sillimanite (fibrolite) and cordierite inclusions in magmatic garnet suggests that the garnet was not produced by assimilation of meta-sedimentary country rocks. Also, the  $\delta^{18}\text{O}$  values of garnet in the pluton (8.3–8.7‰) are significantly lower than  $\delta^{18}\text{O}$  values of garnet in the metapelitic rocks (12.5–13.1‰). Amphibole-plagioclase and garnet-biotite thermometers indicate crystallization temperatures of 708°C and 790°C, respectively. A temperature of 692°C obtained by quartz-garnet oxygen isotope thermometry points to a closure temperature for oxygen diffusion in garnet. The composition of epidote ( $X_{\text{ep}}$ ) and garnet ( $X_{\text{adr}}$ ) indicates ~800°C for the crystallization temperature of these minerals. Elevated andradite content in the rims of garnet suggests that oxygen fugacity increased during crystallization.

**Keywords:** garnet; oxygen isotopes; diorite-tonalite-granodiorite; Iran

### Introduction

Garnet is a common mineral in metamorphic rocks, but it is rare in igneous rocks, and its origin in igneous rocks is controversial. Garnet in granitoids is generally reported from S-type granitoids (e.g. Jung *et al.* 2001; Dahlquist *et al.* 2007; Villaros *et al.* 2009; Taylor and Stevens 2010), but some examples have been found in A-type (e.g. Zhang *et al.* 2009; Zhang *et al.* 2012) and I-type granitoids (e.g. Green 1992; Yuan *et al.* 2008). Most occurrences of magmatic garnet are in felsic pegmatites ( $\text{SiO}_2 \geq 70$  wt.%) associated with peraluminous to metaluminous granitoids (e.g. Allan and Clarke 1981; Miller and Stoddard 1981; du Bray 1988; Hogan 1996; Dahlquist *et al.* 2007). Garnet may occur in granite for several reasons, for example as a restite mineral or xenocryst, as a partial melting product, and as primary magmatic or secondary metasomatic phases (Clarke and Rottura 1994). Kawabata and Takafuji (2005) classified garnet from calc-alkaline rocks of the Setouchi volcanic belt in Japan into I-type garnet (i.e. phenocrysts precipitated from peraluminous magmas at pressures greater than 5–7 kbar) and M-type garnet (metamorphic xenocrysts derived from crustal xenoliths). Therefore, garnet-bearing granitoids can provide useful information concerning melt formation and transportation (e.g. Harangi *et al.* 2001).

In order to understand the magmatic *versus* xenocrystic origin of garnet in igneous rocks (magmatic or xenocrystic), major and trace elements as well as isotopic compositions of garnet and host rock, the nature of mineral inclusions in the garnet, and the pressure-temperature conditions of garnet formation all need to be considered (e.g. Spear 1993; Harangi *et al.* 2001; Kawabata and Takafuji 2005; Dahlquist *et al.* 2007; Yuan *et al.* 2008). For example, garnet composition, its inclusions, and enclosed metamorphic rock fragments provide evidence for xenocrystic garnet in magma (e.g. Harangi *et al.* 2001). Although oscillatory chemical zoning is known to be a characteristic of xenocrystic garnets (e.g. Green and Ringwood 1968; Manning 1983; Harrison 1988), oscillatory chemical zoning is also common in garnets of magmatic origin (e.g. Kano 1983; Day *et al.* 1992). The oxygen isotopic composition of garnet is of potential importance (Lackey *et al.* 2006, 2008) in determining the origin of garnet in granitic rocks, because the closure temperature for oxygen diffusion in garnet is high (>800°C) (e.g. Farquhar *et al.* 1996; Lackey *et al.* 2006, 2008; Harris and Vogeli 2010), hence the  $\delta^{18}\text{O}$  value for garnet does not change once crystallized. Garnet is also highly resistant to post-crystallization interaction to fluids. A number of recent studies have been made on the

\*Corresponding author. Email: [rsamadi@hotmail.com](mailto:rsamadi@hotmail.com)

O-isotope composition of magmatic garnet in granitoids (e.g. Mason *et al.* 1996; Harangi *et al.* 2001; King and Valley 2001; Lackey *et al.* 2006, 2008, 2012; Harris and Vogeli 2010). The  $\delta^{18}\text{O}$  value for magmatic garnet in almandine-bearing dacite and andesite from the northern Pannonian Basin (with mantle origin) is +6.1 to +7.3‰ (Harangi *et al.* 2001). The  $\delta^{18}\text{O}$  values for garnet in the S-type Peninsula granite (South Africa) vary from +10.0 to +11.4‰, suggesting formation by incongruent melting of metapelitic rocks (Harris and Vogeli 2010). Metamorphic garnet in metapelites generally has high  $\delta^{18}\text{O}$  values, ranging from +11.4 to +13.4‰ (Kohn *et al.* 1997).

The Dehnow diorite-tonalite-granodiorite pluton (DTG) is located in NW Mashhad, NE Iran (Figure 1A). Granitoid outcrops are covered by Quaternary gravel fan deposits (Figure 1B), such that outcrops are few but widely distributed. Megacrysts of garnet (~10–20 mm) are a common minor constituent in the DTG pluton. Moazez-Lesco and Plimer (1979) and Plimer and Moazez-Lesco (1981) suggested that all large megacrysts are xenocrysts representing residual phases formed by assimilation of garnet-rich

metamorphic rocks, but did not consider alternative hypotheses. In this paper, we consider the petrology, major elements, and oxygen isotope composition of garnet megacrysts, the major element composition of their inclusions, and coexisting minerals from the Dehnow DTG suite in NE Iran. We also provide a comparison with garnet from granitoids elsewhere around the world in order to further understand the origin of garnets in an I-type granitoid melt and their petrogenetic implications. Abbreviations of minerals were adopted from Kretz (1983) and Whitney and Evans (2010).

### Geological background

The DTG pluton outcrop is approximately 1 km by 2 km in size (Figure 1B) and intruded along the Palaeo-Tethys suture zone. It is a part of the Mashhad-Pamir Arc (so-called Silk Road Arc), which lies in the middle of the Alpine-Himalayan orogenic system. The Silk Road Arc extends 8300 km along the entire southern margin of Eurasia from North China to Europe, and was formed as

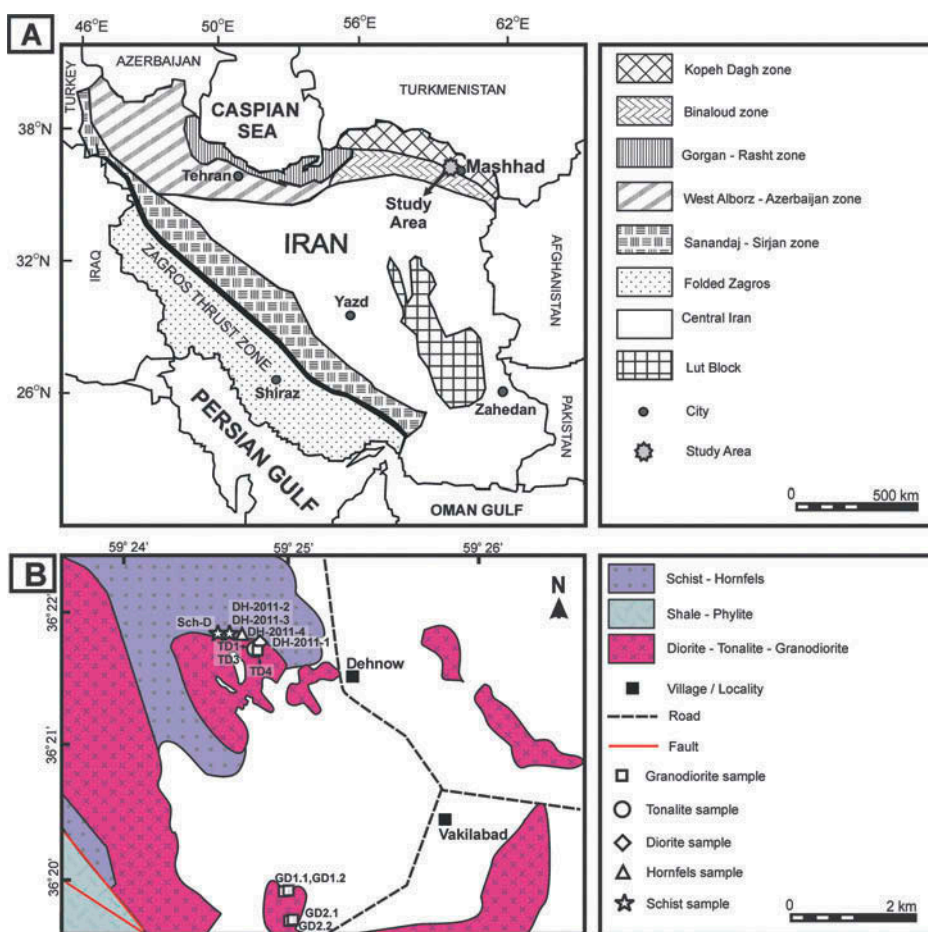


Figure 1. (A) Simplified geological map and main structural zones of Iran. The study region is in NE Iran, NW of Mashhad city (modified geological map of Nabavi 1976); (B) geological map of Dehnow in NW Mashhad (modified after Alavi 1991).

the result of north-dipping subduction of the Palaeo-Tethys (Natalin and Sengör 2005). This suture zone includes meta-ophiolites and meta-flysch sequences, representing the Palaeo-Tethys Ocean closure in the Jurassic (Alavi 1991). It is thought that the Silurian opening of the Palaeo-Tethys in northern Iran followed northward subduction beneath the Turan plate (the southern part of Eurasia) in the Late Devonian and the collision between the Iranian microcontinent and the Turan plate in Late Triassic time (Alavi 1991; Natalin and Sengör 2005). Mineralogical and geochemical works by Samadi (2009) and Samadi *et al.* (2012a, b, 2014), together with the isotopic data of Mirnejad *et al.* (2013) confirm that the Dehnow DTG suite is metaluminous to mildly peraluminous with a calc-alkaline I-type character, and formed after the subduction of the Palaeo-Tethys oceanic slab beneath

the Turan block along the Alpine-Himalayan suture zone. Karimpour *et al.* (2010) suggested that remnants of the Palaeo-Tethys crust (meta-ophiolite and meta-flysch) were intruded by granitic plutons in the Triassic, based on zircon U-Pb dating ( $215 \pm 4$  Ma for the DTG pluton). Meta-ophiolites and granites in the Mashhad area are surrounded by metamorphic rocks consisting of well-layered slate, phyllite, schist, hornfels, marble, quartzite, and skarn. The main lithological units intruded by the DTG pluton are hornfels and mica schist (Figure 1B).

The narrow aureole of hornfels that surrounds the pluton formed from mica schist (Figure 2A). Outside the hornfels aureole, mica schist occurs with a considerable topographic relief relative to the pluton (Figure 2A). Sampling for this work was done from the DTG pluton, the hornfels, and mica schist.



Figure 2. (A) Outcrop of garnet-bearing hornfels and adjacent mica schist. The boundaries of rock units are marked with dashed lines. The view is northward; (B), (C) and (D) outcrop and hand specimens of garnet-bearing diorite-tonalite-granodiorite (DTG) from Dehnow, in which coarse-grained garnet crystals (~10–20 mm in diameter) are visible; (E) hand specimens of garnet-bearing hornfels; (F) hand specimens of garnet-bearing mica schist.

### Analytical techniques

Major-element oxides in the minerals were investigated using a wavelength-dispersive electron probe microanalyzer, JEOL JXA-8800, at the Japan Agency for Marine-Earth Science and Technology (JAMSTEC). The operating conditions were 15 kV accelerating voltage and 15 nA beam current. Standard ZAF data corrections were performed. Natural and synthetic minerals of known composition were used as standards.

Whole-rock major element concentrations ( $\text{SiO}_2$ ,  $\text{TiO}_2$ ,  $\text{Al}_2\text{O}_3$ ,  $\text{MnO}$ ,  $\text{MgO}$ ,  $\text{CaO}$ ,  $\text{K}_2\text{O}$ ,  $\text{Na}_2\text{O}$ ,  $\text{P}_2\text{O}_5$ ) and selected trace elements were measured by X-ray fluorescence (XRF) at Activation Laboratories (ActLabs) and at the XRF laboratory of the Geological Survey of Iran. In general, the limit of detection is about 0.01 wt.% for the major elements (but 0.001% for  $\text{MnO}$ ). The error for standards BIR-1a, W-2, and J-1 run with samples is better than 5% relative to the certified values for trace elements, and better than 1% for major element data (with the exception of  $\text{Na}_2\text{O}$  and  $\text{MnO}$ , which yield errors better than 3%).

For oxygen isotope measurements, the whole-rock samples were disaggregated in a small stainless steel crusher, sieved, and cleaned in hot HCl and ethanol. Garnet and quartz grains were hand-picked. All O-isotope data were obtained at the University of Cape Town. Powdered whole-rock samples were analysed, following methods described by Harris and Ashwal (2002). Approximately 10 mg of sample was reacted with  $\text{ClF}_3$  in externally heated Ni reaction vessels. The liberated  $\text{O}_2$  was converted to  $\text{CO}_2$  using a hot, platinized carbon rod. The quartz, garnet, and biotite grains were analysed by the laser fluorination method described by Harris and Vogeli (2010). Each sample was reacted in the presence of approximately 10 kPa  $\text{BrF}_5$ . The purified  $\text{O}_2$  was then collected on a 5 Å molecular sieve in a glass storage bottle. All isotope ratios were measured using a Finnigan Delta XP mass spectrometer in dual-inlet mode. The estimated precision is 0.16‰ (2 $\sigma$ ) for the conventional and 0.16‰ (2 $\sigma$ ) for the laser data, based on multiple analyses of the internal MQ (quartz) and MON GT (garnet) standards.

### Petrography

The DTG pluton has a granular texture and is composed mainly of plagioclase, quartz, biotite, and accessory minerals which include alkali feldspar, amphibole, garnet, epidote, and ilmenite (Figure 3A, Table 1). Secondary minerals such as muscovite and chlorite were formed by later metamorphism and alteration activity.

Euhedral to subhedral megacrysts of garnet are common in the DTG pluton. The garnet megacrysts range between ~10 and 20 mm in diameter (Figure 2B–D) and contain inclusions of biotite, amphibole, quartz, plagioclase, muscovite, epidote, and ilmenite (Figure 3B).

The hornfels aureole is composed of fine-grained quartz, feldspar, muscovite, garnet, and lesser amounts of biotite, fibrolite, chlorite, tourmaline, and andalusite, and ilmenite. Subhedral to anhedral garnet porphyroblasts (~1.0–1.5 mm) (Figure 2E) contain minute inclusions of quartz, mica, and ilmenite (Figure 3C, D). Outside the aureole, away from the DTG pluton, mica schist contains quartz, muscovite, alkali feldspar, biotite, garnet, and andalusite, and minor amounts of fibrolite, chlorite, ilmenite, and tourmaline. Garnet occurs as small, brownish grains with a diameter of ~1.0–2.5 mm (Figure 2F), and contains minute inclusions of quartz and muscovite (Figure 3E, F).

### Mineral chemistry

In the DTG pluton, plagioclase inclusions in garnet are not albited and have higher anorthite content than phenocrysts in the matrix. The plagioclase in the metamorphic rock is more sodic (Table 2). Amphibole occurs in the matrix and as inclusions in garnet. The amphibole ranges from ferro-hornblende to ferro-tschermarkite hornblende (Table 3, Figure 4A). Epidote inclusions in the garnets and epidote in the matrix have  $X_{\text{ep}} (= \text{Fe}^{3+}/(\text{Fe}^{3+} + \text{Al}^{\text{VI}}))$  of 0.32 and 0.24, respectively. The biotite in the matrix of the DTG pluton and biotite inclusions in the garnet show similar composition, but differ from the biotite in the hornfels and mica schist in having lower Mg# and higher Al<sup>VI</sup> (Tables 4 and 5, Figure 4B).

The garnet megacrysts in the DTG pluton are Fe-rich, having the chemical formula  $\text{alm}_{58.86-65.50} \text{grs}_{13.17-23.11} \text{prp}_{8.18-21.32} \text{sps}_{2.70-9.88} \text{adr}_{0.00-2.47}$  (Table 6). In contrast, the small garnet grains in hornfels and mica schist are enriched in Fe and Mn and depleted in Ca and Mg content (sps value is higher than prp and grs) relative to the garnet in the granitoids of DTG. The chemical formulas of garnet in hornfels and mica schist are  $\text{alm}_{76.84-81.66} \text{sps}_{8.97-14.32} \text{prp}_{5.37-8.26} \text{grs}_{0.50-1.42}$  and  $\text{alm}_{82.07-85.06} \text{sps}_{5.78-9.86} \text{prp}_{5.07-8.46} \text{grs}_{0.56-1.38}$ , respectively (Tables 7 and 8). Figure 5 presents zoning patterns in three garnet megacrysts selected from the DTG pluton. Trend lines are drawn to clarify the complex zoning patterns. Garnet megacrysts show chemical zoning from core to rim of increasing Mg and decreasing Ca, Fe, and Mn (Figure 5). The variation in Fe and Mn is relatively small (<5 mol%), whereas the range is relatively significant for Ca and Mg (>5 mol%). In the hornfels and mica schist, garnet rims (relative to cores) have higher concentrations of Fe and Mg and lower Mn, while the opposite is true for garnet of the DTG pluton (Figure 5).

### Whole-rock chemistry

The whole-rock chemistry of representative samples from the Dehnow DTG pluton and its surrounding metapelitic rocks is given in Table 9. The  $\text{SiO}_2$  content ranges from 55

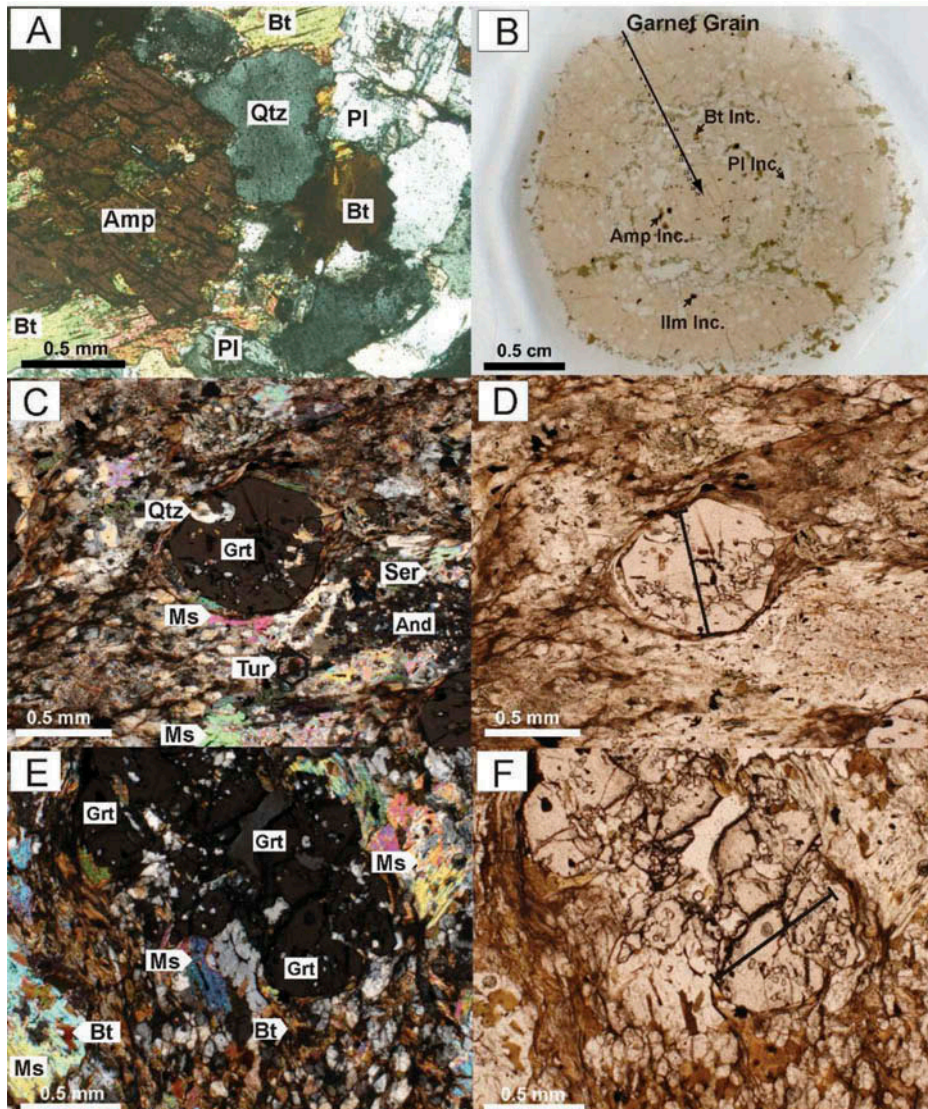


Figure 3. (A) photomicrograph of the Dehnow DTG pluton consisting of amphibole, biotite, quartz, and plagioclase (XPL = cross-polarized light). (B) Garnet megacryst that is uniform in colour and contains minute inclusions of other minerals including plagioclase, amphibole, biotite, and ilmenite. (C) and (D) Garnet in hornfels. The garnet is surrounded by quartz, feldspar, muscovite, andalusite, fibrolite, staurolite, tourmaline, and ilmenite in XPL and PPL (plane-polarized light), respectively. (E) and (F) Garnet in mica schist surrounded by biotite, muscovite, and andalusite in XPL and PPL, respectively. The solid line indicates the analysis profile of garnet.

Table 1. Average modal composition of the DTG pluton.

Rock type	Diorite	Tonalite	Granodiorite
Plagioclase	~45	~39	~43
Quartz	~12	~27	~23
Biotite	~20	~19	~13
Alkali feldspar	~10	~6	~14
Amphibole	~8	~5	~4
Garnet, ilmenite	<5–10 vol.%	<5–10 vol.%	<5–10 vol.%

to 59 wt.% in diorite, from 60 to 64 wt.% in tonalite, and from 65 to 67 wt.% in granodiorite. All of these variants are metaluminous with an alumina saturation index (A/CNK)

of 0.9–1.0 (Table 9). However, part of the DTG pluton contains neither metamorphic garnet-bearing enclaves nor assimilated metamorphic minerals, differing chemically from the adjacent metapelitic rocks in regard to major elements. The DTG pluton is lower in  $\text{Al}_2\text{O}_3$ ,  $\text{Fe}_2\text{O}_3$ ,  $\text{TiO}_2$ , LOI, and A/CNK than the enclosing metamorphic rock, and higher in  $\text{MgO}$ ,  $\text{CaO}$ ,  $\text{Na}_2\text{O} + \text{K}_2\text{O}$ , and  $\text{P}_2\text{O}_5$ .

The oxygen isotope data for the whole-rock, garnet, and quartz of the DTG pluton, hornfels, and mica schist are presented in Table 10. For the hornfels the  $\delta^{18}\text{O}_{\text{garnet}}$  is 13.1‰ ( $n = 1$ ), while for the mica schist the  $\delta^{18}\text{O}_{\text{bulk-rock}}$  value ranges from 14.8 to 16.0‰ (mean<sub>(n=3)</sub> = 15.57, SD = 0.67) and the  $\delta^{18}\text{O}_{\text{garnet}}$  from 12.5 to 13.8‰

Table 2. Representative microprobe analyses of feldspar in the Dehnow DTG pluton (feldspar in the matrix and feldspar inclusions in the garnet), hornfels, and mica schist and the calculated structural formula based on eight oxygen atoms.

Rock type	DTG pluton								Hornfels								Mica schist							
	Inclusions				Matrix																			
Point no.	609	618	619	620	621	622	584	585	586	592	593	85	86	87	183	766	767	768	770					
SiO <sub>2</sub>	59.80	52.78	52.27	56.22	60.64	56.21	51.43	53.14	56.62	57.54	55.33	63.50	64.66	64.18	65.18	64.26	64.68	64.62	64.96					
TiO <sub>2</sub>	0.03	0.02	0.02	0.00	0.00	0.02	0.02	0.00	0.02	0.01	0.00	0.01	0.00	0.00	0.00	0.02	0.00	0.08	0.00					
Al <sub>2</sub> O <sub>3</sub>	24.63	29.91	30.07	27.59	24.70	27.10	30.86	29.31	26.96	26.59	27.91	22.37	22.28	21.63	20.96	21.80	21.44	21.16	21.55					
Cr <sub>2</sub> O <sub>3</sub>	0.01	0.00	0.01	0.00	0.00	0.00	0.00	0.00	0.02	0.01	0.00	0.00	0.00	0.00	0.00	0.00	0.00	0.00	0.00					
FeO	0.83	0.10	0.07	0.06	0.02	0.25	0.31	0.06	0.09	0.39	0.15	0.16	0.14	0.20	0.30	0.50	0.29	0.38	0.22					
MnO	0.02	0.00	0.00	0.01	0.00	0.00	0.00	0.00	0.00	0.01	0.00	0.01	0.00	0.00	0.00	0.01	0.03	0.00	0.01					
MgO	0.19	0.01	0.01	0.01	0.01	0.01	0.01	0.01	0.00	0.00	0.03	0.01	0.05	0.04	0.00	0.02	0.06	0.00	0.04	0.01				
CaO	6.39	12.18	12.66	9.46	5.95	9.02	13.11	9.11	8.55	10.15	9.99	2.39	2.37	1.40	2.25	1.90	1.71	1.89						
Na <sub>2</sub> O	7.97	4.64	4.46	6.09	8.18	6.39	3.98	4.98	6.35	6.82	5.73	10.18	9.38	10.40	10.76	9.89	10.66	10.71	10.61					
K <sub>2</sub> O	0.20	0.07	0.06	0.09	0.11	0.12	0.05	0.06	0.10	0.14	0.07	0.82	0.09	0.07	0.05	0.14	0.07	0.12	0.09					
Sum	100.08	99.70	99.63	99.54	99.60	99.12	99.77	99.28	100.06	99.36	98.09	98.99	98.86	98.67	98.92	99.08	98.82	99.35						
Si	2.67	2.40	2.38	2.54	2.71	2.55	2.34	2.42	2.56	2.58	2.51	2.85	2.86	2.86	2.90	2.86	2.88	2.88	2.88					
Ti	0.00	0.00	0.00	0.00	0.00	0.00	0.00	0.00	0.00	0.00	0.00	0.00	0.00	0.00	0.00	0.00	0.00	0.00	0.00					
Al	1.30	1.60	1.47	1.30	1.45	1.66	1.57	1.44	1.41	1.49	1.18	1.16	1.14	1.10	1.10	1.14	1.12	1.11	1.12					
Cr	0.00	0.00	0.00	0.00	0.00	0.00	0.00	0.00	0.00	0.00	0.00	0.00	0.00	0.00	0.00	0.00	0.00	0.00	0.00					
Fe	0.03	0.00	0.00	0.00	0.00	0.01	0.01	0.00	0.01	0.01	0.01	0.01	0.01	0.01	0.01	0.01	0.01	0.01	0.01					
Mn	0.00	0.00	0.00	0.00	0.00	0.00	0.00	0.00	0.00	0.00	0.00	0.00	0.00	0.00	0.00	0.00	0.00	0.00	0.00					
Mg	0.01	0.00	0.00	0.00	0.00	0.00	0.00	0.00	0.00	0.00	0.00	0.00	0.00	0.00	0.00	0.00	0.00	0.00	0.00					
Ca	0.31	0.59	0.62	0.46	0.28	0.44	0.64	0.57	0.44	0.41	0.49	0.05	0.11	0.11	0.07	0.11	0.09	0.08	0.09					
Na	0.69	0.41	0.39	0.53	0.71	0.56	0.35	0.44	0.56	0.59	0.50	0.89	0.81	0.90	0.93	0.85	0.92	0.93	0.91					
K	0.01	0.00	0.01	0.01	0.01	0.01	0.00	0.01	0.00	0.01	0.00	0.05	0.01	0.00	0.00	0.01	0.01	0.01	0.01					
Sum	5.03	5.01	5.00	5.01	5.01	5.01	5.01	5.01	5.00	5.02	5.00	5.02	4.96	5.02	5.01	5.00	5.02	5.03	5.02					
Albite	0.69	0.41	0.39	0.54	0.71	0.56	0.35	0.43	0.55	0.59	0.50	4.88	12.28	11.16	6.68	11.10	8.92	8.03	8.93					
Anorthite	0.30	0.59	0.61	0.46	0.29	0.44	0.64	0.56	0.44	0.41	0.49	90.31	87.15	88.47	93.02	88.11	90.68	91.30	90.56					
Orthoclase	0.01	0.00	0.00	0.01	0.01	0.01	0.00	0.01	0.00	0.01	0.00	4.81	0.57	0.37	0.31	0.79	0.39	0.66	0.51					

Table 3. Representative microprobe analyses of amphibole in the Dehnow DTG pluto and the calculated structural formula based on 23 oxygen atoms.

Point no.	Garnet grain no.	Inclusions						Matrix					
		605	606	607	608	610	611	612	613	614	616	617	573
SiO <sub>2</sub>	43.56	43.08	43.43	44.37	43.33	42.81	43.05	43.38	42.85	42.28	43.17	43.13	42.30
TiO <sub>2</sub>	1.08	1.11	0.96	0.90	1.07	1.05	1.02	0.99	1.01	1.12	0.99	1.02	1.05
Al <sub>2</sub> O <sub>3</sub>	10.91	11.22	11.35	10.20	11.30	11.16	10.98	10.88	10.84	12.02	10.90	10.90	11.49
Cr <sub>2</sub> O <sub>3</sub>	0.01	0.01	0.04	0.00	0.02	0.00	0.00	0.02	0.00	0.04	0.00	0.02	0.00
FeO	19.90	19.85	19.84	19.29	19.79	20.17	20.01	19.75	19.74	20.46	20.01	20.75	20.50
MnO	0.64	0.66	0.62	0.63	0.66	0.64	0.62	0.62	0.62	0.64	0.64	0.65	0.64
MgO	7.72	7.59	7.68	8.22	7.57	7.43	7.66	8.03	7.97	6.96	7.77	7.30	7.23
CaO	11.44	11.41	11.44	11.56	11.32	11.27	11.31	10.96	11.53	11.16	11.37	11.39	11.45
Na <sub>2</sub> O	0.97	1.11	0.98	0.86	1.12	1.07	1.07	1.34	1.00	1.12	0.99	1.00	0.98
K <sub>2</sub> O	1.11	1.16	1.07	0.89	0.96	1.05	1.04	0.94	0.98	1.02	0.97	1.04	1.17
Sum	97.34	97.20	97.41	96.93	97.13	96.65	96.75	96.92	96.55	96.82	96.83	97.20	96.82
Si	6.59	6.54	6.55	6.71	6.56	6.53	6.55	6.56	6.53	6.44	6.55	6.55	6.46
Al <sup>IV</sup>	1.41	1.46	1.45	1.29	1.44	1.47	1.45	1.44	1.47	1.56	1.45	1.45	1.54
Al <sup>VI</sup>	0.53	0.55	0.57	0.52	0.58	0.53	0.52	0.50	0.48	0.60	0.50	0.51	0.53
Ti	0.12	0.13	0.11	0.10	0.12	0.12	0.12	0.11	0.12	0.13	0.11	0.12	0.12
Cr	0.00	0.00	0.00	0.00	0.00	0.00	0.00	0.00	0.00	0.00	0.00	0.00	0.00
Fe <sub>3+</sub>	0.42	0.39	0.45	0.39	0.43	0.49	0.49	0.49	0.59	0.51	0.53	0.54	0.50
Fe <sub>2+</sub>	2.10	2.13	2.05	2.04	2.07	2.08	2.05	1.90	2.00	2.08	2.00	2.00	2.14
Mn	0.08	0.08	0.08	0.08	0.08	0.08	0.08	0.08	0.08	0.08	0.08	0.08	0.08
Mg	1.74	1.72	1.73	1.85	1.71	1.69	1.74	1.81	1.81	1.58	1.76	1.65	1.65
Ca	1.85	1.86	1.85	1.87	1.84	1.84	1.84	1.77	1.88	1.82	1.85	1.85	1.87
Na	0.28	0.33	0.29	0.25	0.33	0.32	0.31	0.39	0.30	0.33	0.29	0.29	0.29
K	0.21	0.22	0.21	0.17	0.18	0.20	0.20	0.18	0.19	0.20	0.19	0.20	0.23
Sum	15.35	15.41	15.34	15.30	15.35	15.36	15.36	15.35	15.37	15.35	15.33	15.35	15.39
Mg <sup>2+</sup> (Mg <sup>2+</sup> +Fe <sup>2+</sup> )	0.45	0.45	0.46	0.48	0.45	0.45	0.46	0.49	0.47	0.43	0.47	0.44	0.44
Fe <sup>3+</sup> /(Fe <sup>3+</sup> +Al <sup>VI</sup> )	0.44	0.41	0.44	0.43	0.43	0.48	0.49	0.54	0.52	0.47	0.52	0.5	0.48
Naming	FH	FH	FH	FH	FH	FH	FH	FH	FH	FTH	FH	FH	FTH
Barometry method													
P (kbar)													
HZ86	5.9	6.2	6.2	5.2	6.2	6.2	6.0	5.8	5.9	6.9	5.9	5.9	6.5
H87	6.2	6.6	5.5	6.6	6.6	6.4	6.2	7.4	6.2	6.2	6.3	6.3	6.9
JR89	4.8	5.0	4.2	5.1	5.0	4.9	4.7	4.8	5.7	4.8	4.8	4.8	5.3
S92	6.3	6.6	5.6	6.6	6.5	6.4	6.2	7.3	6.3	6.3	6.3	6.3	6.8

Note: FH, ferro-hornblende; FTH, ferro-tschemakitic hornblende; HZ86, Hammarstrom and Zen (1986); H87, Hollister et al. (1987) and Johnson and Rutherford (1989); S92, Schmidt (1992).

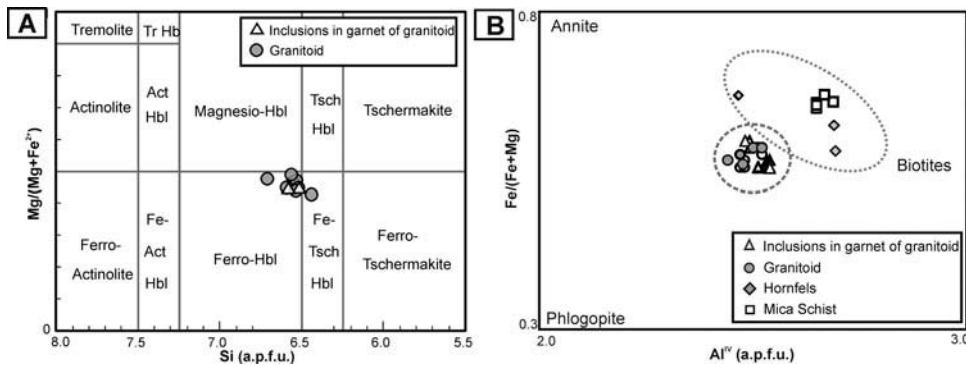


Figure 4. Classification diagrams for (A) amphibole (Leake *et al.* 2004); (B) biotite (after Deer *et al.* 1992). Samples include the Dehnow tonalite, hornfels, mica schist, and inclusions in the garnet of the DTG pluton.

(mean<sub>(n=5)</sub> = 13.00, SD = 0.49). These values are within the compositional range of sedimentary rocks of supercrustal origin (Taylor and Sheppard 1986). In contrast, the  $\delta^{18}\text{O}$  values of garnet from the DTG pluton range from 8.3 to 8.7‰ (mean<sub>(n=7)</sub> = 8.54, SD = 0.13) and the  $\delta^{18}\text{O}$  values of quartz from 11.5 to 12.2‰ (mean<sub>(n=3)</sub> = 12.56, SD = 0.35), with one value of 14.73‰. Assuming a value for  $\Delta_{\text{quartz-magma}}$  of 1.1‰ for granites, as suggested by Fourie and Harris (2011), the original DTG magma had approximate  $\delta^{18}\text{O}$  values of 10.4 to 10.7, 11.1, and 13.6‰, which is consistent with I-type granitoids (e.g. Harris *et al.* 1997; Boztug and Arehart 2007; Öztürk *et al.* 2012) (Figure 6). Combining the quartz-garnet fractionation factor ( $\Delta_{\text{quartz-garnet}} = 2.00$  at 1000 °C, Zheng 1993) with the quartz-magma fractionation factor of 0.4 (Bindeman 2008) gives a garnet-magma fractionation of -1.6‰. This suggests that the average  $\delta^{18}\text{O}$  of the magma ranges between 9.9 and 10.3‰.

## Discussion

### Factors controlling the chemical zoning of garnet in the DTG pluton and country rocks

The parameters that control the chemical zoning in the DTG garnet are pressure (P), temperature (T), growth rate, and changes in the chemical composition of the matrix in equilibrium with the garnet, as suggested by Spear (1993) and Konrad-Schmolke *et al.* (2005) for other localities. Oscillatory compositional zoning is regarded as characteristic of garnet xenocrysts of metamorphic origin (e.g. Green and Ringwood 1968; Manning 1983; Harrison 1988); however, such zoning is also reported in magmatic garnet (e.g. Kano 1983; Day *et al.* 1992; Kawabata and Takafuji 2005). Table 11 summarizes the characteristics of magmatic garnet from several worldwide case studies. In general, garnet phenocrysts are enriched in Fe, except in mafic rocks (e.g. Aydar and Gourgaud 2002; Kawabata and Takafuji 2005; Patranabis-Deb *et al.* 2009). Fe-rich rims and Mg-rich cores are the typical zoning pattern in

magmatic garnet (e.g. Green and Ringwood 1968; Brousse *et al.* 1972; Bach *et al.* 2012), but the opposite may also occur (e.g. Fitton 1972; type 1B and 4 in Harangi *et al.* 2001; type I in Kawabata and Takafuji 2005; Yuan *et al.* 2008; sample 1C in Bach *et al.* 2012). Some garnet phenocrysts in igneous rocks are not zoned (e.g. Aydar and Gourgaud 2002; Mirnejad *et al.* 2008; Patranabis-Deb *et al.* 2009). Moreover, some phenocrysts have Mn-rich rims while others have Ca-rich rims (e.g. Green and Ringwood 1968; Brousse *et al.* 1972; Harangi *et al.* 2001; Kawabata and Takafuji 2005; Yuan *et al.* 2008; Bach *et al.* 2012; Zhang *et al.* 2012). Abbott (1985) attributed the late appearance of Mn-rich garnet during fractional crystallization to strong partitioning of Mn<sup>2+</sup> into the liquid relative to muscovite or biotite.

The Dehnow DTG garnet differs from the metamorphic garnet in the zoning profiles, and in core-to-rim values for Mn, Mg, Ca, and Fe. This places emphasis on the implication that DTG garnet underwent different nucleation and chemical growth to those in the surrounding metamorphic rocks. The Mg and Ca zoning in the DTG garnet (Figure 5A, B, C) is elaborated more than in the fine garnet grains of the mica schist and hornfels (Figure 5D, E). Based on polynomial trendline patterns, the garnet in the DTG granitoids has a more pronounced negative Ca–Mg correlation, with a core-to-rim increase in Mg and decrease in Fe and Ca (Figure 5A, B, C). These zoning patterns resemble the zoning patterns described by Hamer and Moyes (1982); Brousse *et al.* (1972, sample C), Harangi *et al.* (2001, type 2) and Bach *et al.* (2012, samples 1A and 1B). With regard to the varieties of magmatic garnet described by Dahlquist *et al.* (2007), garnet megacrysts from the DTG pluton show distinctive U-shaped or irregular zoning in terms of Mn (Figure 5). The oscillatory zoning of Fe, Ca, and Mg may be an indicator of variation in melt composition (Day *et al.* 1992; Kawabata and Takafuji 2005) and P<sub>H2O</sub> (Kano and Yashima 1976) during garnet growth.

Table 4. Representative microprobe analyses of biotite in the Dehnow DTG pluton and biotite inclusions in the garnet (DH1A, garnet grain b3) and the calculated structural formula based on 22 oxygen atoms.

Point no.	Inclusions										Matrix									
	432	434	442	451	452	482	586	587	594	557	558	559	560	561	562	563	564	566	567	568
SiO <sub>2</sub>	35.57	35.74	35.51	36.68	35.71	33.02	35.52	35.39	35.64	35.49	35.76	35.50	36.19	35.18	35.70	35.79	35.43	35.73	36.08	
TiO <sub>2</sub>	1.33	1.40	1.53	1.18	1.30	0.90	2.16	2.34	3.02	2.85	1.85	2.95	2.49	1.93	2.15	3.03	2.86	2.08	1.63	
Al <sub>2</sub> O <sub>3</sub>	18.25	18.62	18.59	19.83	19.07	18.71	17.87	17.58	17.46	16.28	16.59	16.79	16.35	16.37	16.89	16.54	16.18	16.29	16.75	17.10
Cr <sub>2</sub> O <sub>3</sub>	0.01	0.02	0.00	0.00	0.00	0.00	0.02	0.00	0.00	0.00	0.00	0.01	0.01	0.00	0.00	0.04	0.00	0.00	0.00	0.01
FeO	22.38	22.38	22.51	21.28	22.66	25.94	23.32	23.31	23.15	22.58	21.92	21.47	22.21	21.68	21.59	21.53	21.94	22.05	21.64	21.72
MnO	0.31	0.26	0.26	0.24	0.30	0.27	0.26	0.24	0.28	0.41	0.40	0.33	0.35	0.35	0.40	0.39	0.38	0.41	0.33	0.34
MgO	7.78	7.72	7.23	6.70	7.05	6.79	6.67	6.65	6.64	8.02	8.00	8.69	8.26	8.32	8.82	8.60	8.10	7.90	8.59	8.96
CaO	0.13	0.11	0.74	0.18	0.22	0.57	0.04	0.03	0.06	0.02	0.04	0.12	0.07	0.09	0.07	0.03	0.04	0.15	0.00	0.07
Na <sub>2</sub> O	0.09	0.20	0.11	0.28	0.21	0.60	0.16	0.04	0.09	0.08	0.10	0.08	0.10	0.07	0.07	0.08	0.08	0.08	0.07	0.05
K <sub>2</sub> O	8.81	9.50	9.06	9.53	9.37	6.44	9.46	9.57	9.48	9.24	9.09	8.92	9.07	8.92	9.27	9.16	8.98	9.33	9.26	9.47
Sum	94.66	95.94	95.55	95.90	95.91	93.23	95.48	95.15	95.13	95.26	94.49	94.04	94.84	94.49	94.23	94.20	94.51	94.48	94.45	95.44
Si	5.47	5.43	5.43	5.50	5.43	5.27	5.46	5.47	5.49	5.47	5.48	5.52	5.47	5.55	5.46	5.51	5.52	5.49	5.51	5.50
Al <sup>IV</sup>	2.53	2.57	2.50	2.57	2.73	2.54	2.53	2.51	2.53	2.52	2.48	2.53	2.45	2.49	2.49	2.51	2.49	2.49	2.50	
Al <sup>VI</sup>	0.77	0.77	0.77	1.01	0.85	0.79	0.70	0.67	0.67	0.43	0.50	0.58	0.44	0.51	0.55	0.53	0.45	0.47	0.55	0.56
Ti	0.15	0.16	0.18	0.13	0.15	0.11	0.25	0.27	0.27	0.35	0.33	0.21	0.34	0.29	0.23	0.25	0.35	0.33	0.24	0.19
Cr	0.00	0.00	0.00	0.00	0.00	0.00	0.00	0.00	0.00	0.00	0.00	0.00	0.00	0.00	0.00	0.00	0.00	0.00	0.00	
Fe	2.88	2.84	2.88	2.67	2.88	3.46	3.00	3.01	2.99	2.91	2.83	2.77	2.86	2.78	2.80	2.78	2.83	2.86	2.79	2.77
Mn	0.04	0.03	0.03	0.04	0.04	0.03	0.04	0.03	0.04	0.05	0.05	0.04	0.05	0.05	0.05	0.05	0.05	0.05	0.04	0.04
Mg	1.78	1.75	1.65	1.50	1.60	1.62	1.53	1.53	1.53	1.84	1.84	2.00	1.90	2.04	1.98	1.98	1.86	1.82	1.97	2.03
Ca	0.02	0.02	0.12	0.03	0.04	0.10	0.01	0.01	0.01	0.01	0.01	0.02	0.01	0.01	0.01	0.01	0.01	0.01	0.01	0.01
Na	0.03	0.06	0.03	0.08	0.06	0.18	0.05	0.01	0.03	0.03	0.03	0.02	0.02	0.02	0.02	0.02	0.02	0.02	0.02	0.02
K	1.73	1.84	1.77	1.82	1.31	1.86	1.89	1.86	1.81	1.79	1.76	1.78	1.75	1.83	1.81	1.76	1.84	1.82	1.84	
Sum	15.81	15.91	15.82	15.86	15.61	15.82	15.80	15.61	15.82	15.78	15.85	15.80	15.82	15.87	15.86	15.78	15.81	15.87	15.96	
Fe/Fe+Mg	0.62	0.62	0.64	0.64	0.68	0.66	0.66	0.66	0.66	0.61	0.58	0.60	0.59	0.58	0.58	0.60	0.61	0.59	0.58	

Table 5. Representative microprobe analyses of biotite inclusions in the garnet of Dehnnow hornfels and mica schist and the calculated structural formula based on 22 oxygen atoms.

Rock type	Mica schist						Hornfels												
	553			555a			586	587											
Grt grain no.	764	765	769	772	773	798	806	811	813	814	815	816	823	829	836	855	875	168	221
SiO <sub>2</sub>	33.91	33.44	34.71	33.75	34.36	34.17	34.39	34.15	34.19	33.93	34.23	34.22	34.78	34.19	34.39	34.50	34.81	34.70	
TiO <sub>2</sub>	1.87	1.79	1.65	1.81	1.99	2.20	1.75	1.75	1.90	1.82	1.82	1.86	1.69	1.97	1.61	1.97	1.85	1.61	1.86
Al <sub>2</sub> O <sub>3</sub>	20.04	20.56	20.33	19.70	19.99	19.75	19.49	20.64	20.35	20.20	20.03	20.20	19.94	20.05	20.39	20.00	20.46	20.78	20.10
Cr <sub>2</sub> O <sub>3</sub>	0.04	0.05	0.03	0.01	0.02	0.01	0.03	0.01	0.06	0.04	0.05	0.06	0.02	0.01	0.06	0.03	0.01	0.09	0.11
FeO	23.18	24.01	22.81	23.63	23.47	23.42	23.09	22.13	23.33	24.04	23.71	23.78	23.83	23.25	23.42	23.13	23.16	21.02	22.70
MnO	0.04	0.06	0.05	0.07	0.06	0.07	0.04	0.06	0.04	0.06	0.04	0.08	0.03	0.11	0.12	0.06	0.04	0.08	0.22
MgO	6.16	6.51	6.35	6.52	6.23	6.25	6.08	6.08	6.22	6.17	5.99	6.10	6.11	5.93	6.23	6.12	6.12	6.67	7.02
CaO	0.10	0.10	0.10	0.12	0.06	0.02	0.06	0.15	0.06	0.16	0.06	0.05	0.05	0.03	0.06	0.03	0.00	0.00	0.05
Na <sub>2</sub> O	0.32	0.33	0.46	0.38	0.35	0.31	0.29	0.34	0.32	0.32	0.27	0.29	0.31	0.29	0.30	0.35	0.32	0.31	0.25
K <sub>2</sub> O	7.90	7.30	7.96	8.04	8.01	8.24	8.06	7.50	7.59	8.08	8.25	8.05	8.01	7.93	8.49	8.47	8.21	8.34	8.46
Sum	93.57	94.15	94.45	94.03	94.54	94.66	93.06	93.08	94.10	94.91	94.14	94.71	94.28	94.33	94.74	94.51	94.78	94.85	95.49
Si	5.31	5.22	5.34	5.28	5.32	5.37	5.35	5.30	5.29	5.30	5.30	5.30	5.32	5.37	5.29	5.31	5.31	5.30	5.30
Al <sup>IV</sup>	2.69	2.78	2.66	2.72	2.68	2.63	2.65	2.70	2.71	2.70	2.70	2.70	2.68	2.63	2.71	2.67	2.69	2.70	2.70
Al <sup>VI</sup>	1.01	1.00	1.03	0.92	0.96	0.92	0.99	1.13	1.02	0.97	0.99	0.98	0.98	1.01	1.02	0.98	1.03	1.02	0.92
Ti	0.22	0.21	0.19	0.21	0.23	0.26	0.21	0.20	0.22	0.21	0.21	0.22	0.20	0.23	0.19	0.23	0.21	0.18	0.21
Cr	0.00	0.01	0.00	0.00	0.00	0.00	0.00	0.01	0.01	0.01	0.01	0.00	0.00	0.00	0.01	0.00	0.00	0.01	0.01
Fe	3.04	3.13	2.94	3.09	3.04	3.03	3.04	2.88	3.03	3.11	3.10	3.08	3.10	3.08	3.00	3.03	3.00	2.98	2.67
Mn	0.01	0.01	0.01	0.01	0.01	0.01	0.01	0.01	0.01	0.01	0.01	0.01	0.02	0.01	0.01	0.01	0.01	0.03	0.03
Mg	1.44	1.51	1.46	1.52	1.44	1.43	1.41	1.44	1.41	1.42	1.39	1.41	1.42	1.36	1.44	1.41	1.41	1.74	1.60
Ca	0.02	0.02	0.02	0.02	0.01	0.00	0.01	0.02	0.03	0.00	0.01	0.01	0.00	0.01	0.00	0.01	0.00	0.01	0.01
Na	0.10	0.10	0.14	0.11	0.11	0.09	0.09	0.10	0.10	0.08	0.08	0.09	0.09	0.09	0.09	0.11	0.10	0.09	0.07
K	1.58	1.45	1.56	1.61	1.58	1.63	1.62	1.49	1.50	1.59	1.64	1.59	1.57	1.56	1.57	1.54	1.67	1.61	1.62
Sum	15.51	15.47	15.60	15.59	15.57	15.58	15.54	15.45	15.49	15.57	15.56	15.57	15.57	15.62	15.60	15.58	15.64	15.66	15.66
Fe/Fe+Mg	0.68	0.67	0.67	0.67	0.68	0.68	0.68	0.67	0.68	0.68	0.68	0.69	0.69	0.69	0.68	0.68	0.68	0.61	0.64

Table 6. Representative microprobe analyses of garnet in the Dehnow DTG pluton and the calculated structural formula based on 12 oxygen atoms.

DHI-grain (nm to core of a garnet phenocryst)																											
sample no.	414	417	420	426	429	432	436	439	442	451	455	458	461	464	468	471	474	477	482	498	501	504	507	513	516	519	522
$\text{Mg}_{\text{f}}$	38.31	37.54	38.70	38.26	38.68	38.16	38.05	38.16	37.94	37.88	38.04	37.85	38.11	37.92	38.02	38.07	37.90	37.60	37.90	37.94	37.92	38.11	38.12	38.03			
$\text{Mg}_{\text{g}}$	0.28	0.35	0.22	0.34	0.20	0.24	0.25	0.20	0.45	0.38	0.40	0.33	0.18	0.55	0.44	0.38	0.39	0.64	0.22	0.52	0.50	0.19	0.54	0.37	0.51	0.42	
$\text{Mg}_{\text{d}}$	21.41	21.02	21.00	21.46	21.39	21.53	20.98	20.96	21.23	21.24	21.19	21.37	21.14	20.95	20.97	21.20	21.04	21.23	21.12	21.26	21.42	21.23	21.13	21.37			
$\text{Mg}_{\text{o}}$	0.00	0.00	0.02	0.00	0.02	0.00	0.01	0.04	0.01	0.04	0.00	0.00	0.01	0.01	0.02	0.03	0.00	0.01	0.00	0.00	0.00	0.00	0.00	0.00	0.00		
$\text{Mg}_{\text{eO}}$	28.02	27.62	27.96	28.39	28.48	28.75	29.15	28.82	28.69	29.27	29.12	29.65	28.56	29.20	28.94	28.91	28.69	28.81	29.59	28.85	28.74	29.51	29.03	29.33	29.64	29.37	
$\text{MnO}$	1.90	2.13	2.11	2.21	2.24	2.28	2.29	2.53	2.31	2.45	1.84	2.06	2.05	1.97	1.90	1.72	1.94	1.92	1.67	1.79	1.75	1.95	1.86	1.73	1.82	1.98	
$\text{MnO}$	5.46	5.32	5.15	4.67	4.35	4.69	4.43	3.94	3.19	2.90	3.42	3.10	3.04	3.19	3.13	3.31	3.27	3.54	3.49	3.53	3.48	3.60	3.50	3.19	3.20	3.25	
$\text{MnO}$	5.11	5.32	5.00	5.30	5.23	5.68	5.27	6.43	6.73	6.63	6.64	6.37	6.82	6.64	7.04	6.84	6.61	6.35	6.79	6.17	6.82	6.94	6.41	6.79			
$\text{MnO}$	0.00	0.00	0.06	0.04	0.04	0.00	0.03	0.01	0.02	0.03	0.01	0.00	0.03	0.00	0.03	0.00	0.03	0.01	0.01	0.01	0.01	0.01	0.01	0.01	0.03		
$\text{MnO}$	0.00	0.05	0.14	0.03	0.01	0.02	0.00	0.00	0.01	0.01	0.00	0.02	0.00	0.00	0.01	0.01	0.02	0.00	0.00	0.00	0.00	0.00	0.00	0.00	0.00		
$\text{MnO}$	100.51	99.37	100.36	100.63	100.61	100.49	101.03	100.29	100.22	100.37	100.69	100.52	100.53	100.40	100.44	100.62	100.46	100.54	100.53	100.49	100.91	100.51	100.49	100.96	100.33		
$\text{MnO}$	2.99	2.97	3.03	3.00	3.02	2.99	2.98	3.01	3.00	2.99	3.01	2.99	3.00	3.00	3.00	3.00	2.99	2.99	2.99	2.99	3.00	2.99	3.00	2.98			
$\text{MnO}$	0.01	0.03	0.00	0.00	0.00	0.01	0.02	0.00	0.00	0.01	0.00	0.01	0.00	0.00	0.00	0.01	0.01	0.01	0.01	0.01	0.01	0.01	0.01	0.02			
$\text{MnO}$	1.96	1.94	1.94	1.97	1.98	1.97	1.97	1.95	1.96	1.98	1.96	1.97	1.99	1.97	1.95	1.95	1.97	1.95	1.96	1.97	1.97	1.96	1.97	1.96			
$\text{MnO}$	0.02	0.02	0.01	0.01	0.02	0.01	0.01	0.01	0.01	0.03	0.02	0.02	0.01	0.03	0.04	0.03	0.02	0.04	0.02	0.03	0.01	0.03	0.02	0.03			
$\text{MnO}$	0.00	0.00	0.00	0.00	0.00	0.00	0.00	0.00	0.00	0.00	0.00	0.00	0.00	0.00	0.00	0.00	0.00	0.00	0.00	0.00	0.00	0.00	0.00	0.00			
$\text{MnO}$	0.02	0.04	0.01	0.00	0.00	0.01	0.02	0.01	0.00	0.01	0.00	0.00	0.01	0.00	0.01	0.02	0.01	0.01	0.02	0.01	0.01	0.01	0.01	0.02			
$\text{MnO}$	1.81	1.79	1.82	1.86	1.87	1.86	1.86	1.91	1.90	1.91	1.92	1.96	1.89	1.92	1.89	1.90	1.88	1.93	1.89	1.94	1.91	1.92	1.94	1.91			
$\text{MnO}$	0.13	0.14	0.14	0.15	0.15	0.15	0.15	0.17	0.15	0.16	0.12	0.14	0.14	0.13	0.13	0.11	0.13	0.12	0.13	0.12	0.12	0.12	0.13	0.12			
$\text{MnO}$	0.64	0.63	0.60	0.55	0.51	0.52	0.46	0.38	0.34	0.40	0.37	0.36	0.38	0.37	0.39	0.38	0.37	0.39	0.38	0.42	0.41	0.42	0.41	0.38	0.39		
$\text{MnO}$	0.43	0.45	0.42	0.44	0.44	0.48	0.45	0.55	0.57	0.56	0.54	0.58	0.56	0.54	0.58	0.56	0.59	0.54	0.57	0.57	0.55	0.58	0.54	0.57			
$\text{MnO}$	0.00	0.00	0.00	0.00	0.00	0.00	0.00	0.00	0.00	0.00	0.00	0.00	0.00	0.00	0.00	0.00	0.00	0.00	0.00	0.00	0.00	0.00	0.00	0.00			
$\text{MnO}$	0.00	0.00	0.00	0.00	0.00	0.00	0.00	0.00	0.00	0.00	0.00	0.00	0.00	0.00	0.00	0.00	0.00	0.00	0.00	0.00	0.00	0.00	0.00	0.00			
$\text{MnO}$	8.00	8.01	7.98	7.99	7.98	8.00	8.01	7.99	7.98	7.99	8.00	7.99	7.98	7.98	7.99	7.99	7.99	8.00	7.99	7.99	7.99	7.99	7.99	7.99			
$\text{MnO}$	0.26	0.26	0.25	0.23	0.21	0.20	0.17	0.15	0.16	0.15	0.17	0.16	0.15	0.17	0.16	0.17	0.18	0.18	0.18	0.18	0.18	0.18	0.18	0.16			
$\text{MnO}$	60.14	58.88	60.35	61.74	63.16	61.79	61.55	63.48	63.74	63.62	64.04	65.37	63.86	62.57	64.33	62.39	62.60	62.64	64.05	62.39	64.33	63.60	63.81	64.65	63.87		
$\text{MnO}$	0.88	1.86	0.61	0.24	0.00	0.52	0.87	0.72	0.19	0.00	0.72	0.07	0.03	0.00	0.50	0.92	0.34	0.43	0.68	1.16	0.86	0.67	0.29	0.47			
$\text{MnO}$	13.46	13.33	13.65	14.73	14.70	14.22	15.09	14.24	18.32	19.21	18.06	18.91	17.99	19.48	18.50	19.24	19.11	18.42	19.12	16.86	18.49	19.07	16.82	19.22	19.21	17.94	
$\text{MnO}$	21.31	21.13	20.54	18.35	17.08	18.39	17.36	15.70	12.80	11.52	13.48	12.33	11.99	12.71	12.52	13.19	12.96	14.11	13.76	13.93	13.80	14.15	13.81	12.69	12.92		
$\text{MnO}$	4.21	4.81	4.78	4.94	5.00	5.08	5.10	5.73	5.27	5.53	4.12	4.65	4.59	4.46	4.52	3.89	4.37	4.35	3.74	4.01	4.46	3.91	4.37	4.21	3.88		
$\text{MnO}$	0.00	0.00	0.06	0.00	0.06	0.00	0.03	0.13	0.03	0.00	0.00	0.03	0.06	0.10	0.00	0.03	0.00	0.10	0.06	0.00	0.00	0.03	0.00	0.00			

(Continued)

Table 6. (Continued).

Sample no.	DH1-grain2 (rim to core of a garnet phenocryst)																									
	267	271	280	292	296	300	309	313	316	326	329	332	335	338	341	344	347	350	353	356	359	362	365	368	371	374
SiO <sub>2</sub>	38.11	38.23	38.41	38.32	38.09	37.93	38.27	38.38	38.70	38.09	38.02	38.12	38.27	37.73	38.12	37.53	38.22	37.98	37.94	37.83	37.94	38.51	37.50			
TiO <sub>2</sub>	0.25	0.24	0.04	0.29	0.14	0.23	0.38	0.36	0.35	0.17	0.26	0.32	0.34	0.43	0.26	0.48	0.39	0.32	0.64	0.20	0.34	0.27	0.37	0.59	1.03	
Al <sub>2</sub> O <sub>3</sub>	21.39	21.64	21.65	21.37	21.52	21.33	21.11	21.31	21.53	21.47	21.29	21.26	21.40	21.23	21.36	21.29	21.21	21.41	21.03	21.39	21.15	21.28	21.09	21.33	21.20	
Cr <sub>2</sub> O <sub>3</sub>	0.00	0.00	0.03	0.00	0.00	0.00	0.00	0.00	0.00	0.00	0.00	0.00	0.00	0.04	0.01	0.00	0.00	0.00	0.00	0.00	0.00	0.00	0.00	0.00		
FeO	28.30	28.63	28.50	28.72	28.74	28.68	28.47	28.27	28.81	29.19	28.61	29.21	29.00	29.46	28.98	29.64	29.63	29.24	29.09	29.34	29.20	29.37	29.48	29.25	29.18	
MnO	1.73	2.20	2.65	2.54	2.36	2.42	2.22	2.01	2.12	2.44	2.59	2.33	2.10	2.21	1.91	2.01	2.03	2.06	2.04	2.03	2.07	2.05	2.05	1.98	1.94	
MgO	5.28	4.45	4.42	4.34	4.75	4.44	4.48	4.47	3.91	3.07	2.99	2.97	3.30	3.17	3.16	3.16	3.32	3.27	3.23	3.17	3.02	3.14	2.99	3.03	3.10	
CaO	5.32	5.31	4.71	5.27	4.89	5.26	5.39	5.76	5.63	5.72	6.93	6.72	6.74	6.49	6.81	6.44	6.16	6.69	6.70	6.52	6.71	6.54	6.77	6.53	6.56	6.81
Na <sub>2</sub> O	0.04	0.02	0.03	0.04	0.04	0.08	0.02	0.01	0.02	0.01	0.00	0.00	0.00	0.01	0.01	0.02	0.01	0.04	0.02	0.00	0.00	0.03	0.01	0.00	0.01	
K <sub>2</sub> O	0.03	0.04	0.00	0.00	0.00	0.01	0.00	0.00	0.00	0.00	0.00	0.01	0.00	0.00	0.00	0.00	0.00	0.01	0.01	0.00	0.00	0.00	0.00	0.00	0.00	
Sum	100.44	100.76	100.41	100.92	100.54	100.38	100.33	100.59	101.63	101.01	100.78	100.97	100.83	100.85	100.82	100.29	100.99	100.80	100.45	100.79	100.68	100.39	100.82	100.45	101.28	100.78
Si	2.98	2.99	3.01	3.00	2.99	3.01	3.01	3.00	2.99	3.00	3.01	2.98	3.00	2.98	3.00	2.98	3.00	2.97	2.99	3.00	2.98	3.00	2.98	3.01	2.96	
Al <sup>IV</sup>	0.02	0.01	0.00	0.00	0.01	0.01	0.00	0.00	0.00	0.01	0.00	0.00	0.00	0.02	0.00	0.00	0.02	0.01	0.03	0.01	0.00	0.02	0.00	0.00	0.04	
Al <sup>VI</sup>	1.96	1.99	2.00	1.97	1.98	1.97	1.96	1.97	1.97	1.98	1.98	1.97	1.96	1.98	1.96	1.97	1.97	1.95	1.98	1.97	1.97	1.97	1.97	1.97	1.93	
Ti	0.01	0.01	0.00	0.02	0.01	0.01	0.02	0.01	0.02	0.02	0.01	0.02	0.02	0.02	0.03	0.02	0.02	0.03	0.02	0.04	0.01	0.02	0.02	0.02	0.06	
Cr	0.02	0.00	0.00	0.00	0.00	0.00	0.00	0.00	0.00	0.00	0.00	0.00	0.00	0.00	0.00	0.00	0.00	0.00	0.00	0.00	0.00	0.00	0.00	0.00		
Fe <sup>3+</sup>	0.02	0.00	0.01	0.01	0.01	0.01	0.01	0.01	0.01	0.01	0.01	0.01	0.01	0.01	0.01	0.01	0.01	0.01	0.01	0.01	0.01	0.01	0.01	0.01		
Fe <sup>2+</sup>	1.83	1.88	1.89	1.88	1.86	1.85	1.86	1.86	1.90	1.88	1.92	1.92	1.92	1.91	1.95	1.95	1.91	1.92	1.92	1.94	1.92	1.94	1.93	1.92		
Mn	0.11	0.15	0.18	0.17	0.16	0.16	0.15	0.13	0.14	0.16	0.17	0.16	0.14	0.15	0.13	0.14	0.14	0.13	0.14	0.14	0.14	0.14	0.14	0.13		
Mg	0.62	0.52	0.51	0.56	0.52	0.52	0.52	0.52	0.52	0.46	0.36	0.35	0.35	0.39	0.37	0.37	0.39	0.38	0.37	0.36	0.37	0.35	0.35	0.36		
Ca	0.45	0.40	0.44	0.41	0.44	0.45	0.48	0.47	0.48	0.59	0.57	0.57	0.55	0.57	0.55	0.56	0.57	0.56	0.57	0.55	0.57	0.55	0.55	0.58		
Na	0.00	0.00	0.00	0.00	0.00	0.00	0.00	0.00	0.00	0.00	0.00	0.00	0.00	0.00	0.00	0.00	0.00	0.00	0.00	0.00	0.00	0.00	0.00	0.00		
K	0.00	0.00	0.00	0.00	0.00	0.00	0.00	0.00	0.00	0.00	0.00	0.00	0.00	0.00	0.00	0.00	0.00	0.00	0.00	0.00	0.00	0.00	0.00	0.00		
Sum	8.00	7.99	7.99	8.00	7.99	7.99	7.99	7.99	8.00	7.99	7.98	8.01	7.98	8.01	7.98	8.01	7.98	8.01	7.99	8.00	7.99	8.00	7.98	7.99		
Mg#	0.25	0.22	0.21	0.21	0.23	0.22	0.22	0.22	0.19	0.16	0.15	0.15	0.17	0.16	0.16	0.17	0.17	0.16	0.16	0.16	0.16	0.16	0.15	0.16		
Almandine	60.54	63.45	62.39	62.41	62.29	61.80	61.46	62.03	63.18	62.44	63.83	64.51	63.57	63.89	64.53	65.38	63.60	63.34	63.83	64.01	64.61	63.86	64.73	64.94		
Andradite	1.14	0.00	0.30	0.41	0.70	0.55	0.21	0.26	0.61	0.42	0.27	0.00	0.96	0.00	0.82	0.00	0.63	0.44	0.65	0.19	0.23	0.86	0.31	0.00	0.28	
Grossular	13.82	14.89	13.29	14.50	13.35	14.16	14.84	16.13	15.54	15.48	19.23	18.83	19.09	17.35	19.28	17.57	17.53	18.37	18.66	17.94	18.79	18.46	18.31	19.18		
Pyrope	17.36	17.35	17.06	18.59	17.45	17.80	17.69	15.30	12.11	11.83	11.70	13.04	12.51	12.55	13.11	12.97	12.86	12.47	12.01	12.37	11.92	11.98	12.32			
Spessartine	3.85	4.88	5.91	5.67	5.25	5.40	5.01	4.71	5.43	5.80	5.24	4.70	4.96	4.28	4.54	4.57	4.29	4.60	4.66	4.54	4.68	4.59	4.64	4.38		
Uvarovite	0.00	0.00	0.00	0.09	0.00	0.00	0.00	0.00	0.00	0.00	0.00	0.00	0.00	0.00	0.00	0.00	0.00	0.00	0.00	0.00	0.00	0.00	0.00	0.00		

(Continued)

Table 6. (Continued).

Table 7. Representative microprobe data (rim to core to rim) of garnet (sample DH-5-grain 587) from Detmow hornfels and the calculated structural formula based on 12 oxygen atoms.

Sample no.	210	211	213	214	215	216	217	218	219	220	222	223	224	225	226	227
SiO <sub>2</sub>	36.87	37.13	37.09	36.97	36.83	37.17	37.13	37.01	36.93	36.66	37.00	37.10	37.26	37.19	37.17	
TiO <sub>2</sub>	0.02	0.04	0.10	0.15	0.20	0.19	0.30	0.14	0.15	0.17	0.15	0.10	0.14	0.11	0.00	0.00
Al <sub>2</sub> O <sub>3</sub>	21.49	21.62	21.40	21.51	21.47	21.49	20.97	21.51	21.36	21.49	21.78	21.40	21.24	21.55	21.30	21.30
Cr <sub>2</sub> O <sub>3</sub>	0.01	0.01	0.04	0.00	0.01	0.00	0.01	0.00	0.00	0.04	0.00	0.00	0.01	0.04	0.00	0.02
FeO	35.60	35.02	35.73	34.89	34.97	34.48	34.79	33.61	33.66	33.74	34.08	33.99	34.55	34.68	35.17	35.37
MnO	4.38	4.30	3.89	4.88	4.75	4.89	5.38	6.05	6.11	6.17	5.50	5.17	4.82	4.68	4.37	4.76
MgO	1.28	1.91	2.04	1.93	1.80	1.90	1.85	1.97	1.74	1.77	1.65	1.88	2.02	1.92	1.93	1.62
CaO	0.17	0.46	0.49	0.43	0.43	0.44	0.34	0.39	0.42	0.40	0.47	0.45	0.47	0.45	0.43	0.18
Na <sub>2</sub> O	0.04	0.01	0.02	0.00	0.03	0.04	0.01	0.04	0.06	0.03	0.01	0.02	0.02	0.01	0.01	0.03
K <sub>2</sub> O	0.00	0.00	0.02	0.00	0.00	0.00	0.01	0.00	0.00	0.00	0.04	0.00	0.00	0.01	0.01	0.00
Sum	99.86	100.51	100.81	100.78	100.48	100.61	100.79	100.71	100.62	100.31	100.40	100.54	100.49	100.43	100.44	100.44
Si	2.99	2.98	2.98	2.97	2.97	2.98	3.00	2.97	2.97	2.97	2.98	2.97	2.97	2.99	3.00	2.98
Al <sup>IV</sup>	0.01	0.02	0.02	0.03	0.03	0.02	0.00	0.03	0.03	0.03	0.03	0.02	0.03	0.01	0.02	0.00
Al <sup>VI</sup>	2.05	2.04	2.01	2.02	2.02	2.02	1.99	2.02	2.02	2.01	2.01	2.04	2.02	2.02	2.03	2.03
Ti	0.00	0.01	0.01	0.01	0.01	0.01	0.01	0.02	0.01	0.01	0.01	0.01	0.01	0.01	0.01	0.00
Cr	0.00	0.00	0.00	0.00	0.00	0.00	0.00	0.00	0.00	0.00	0.00	0.00	0.00	0.00	0.00	0.00
Fe <sup>3+</sup>	0.00	0.00	0.00	0.00	0.00	0.00	0.00	0.00	0.00	0.00	0.00	0.00	0.00	0.00	0.00	0.00
Fe <sup>2+</sup>	2.48	2.40	2.43	2.38	2.40	2.36	2.36	2.30	2.30	2.31	2.31	2.35	2.34	2.36	2.40	2.43
Mn	0.30	0.29	0.26	0.33	0.32	0.33	0.37	0.41	0.42	0.42	0.38	0.35	0.33	0.32	0.30	0.33
Mg	0.15	0.23	0.24	0.23	0.22	0.23	0.22	0.24	0.24	0.21	0.21	0.20	0.22	0.24	0.23	0.19
Ca	0.01	0.04	0.04	0.04	0.04	0.04	0.04	0.03	0.03	0.04	0.03	0.04	0.04	0.04	0.04	0.02
Na	0.00	0.00	0.00	0.00	0.00	0.00	0.00	0.00	0.00	0.00	0.00	0.00	0.00	0.00	0.00	0.00
K	0.00	0.00	0.00	0.00	0.00	0.00	0.00	0.00	0.00	0.00	0.00	0.00	0.00	0.00	0.00	0.00
Sum	8.00	8.00	8.01	8.00	8.00	7.99	8.00	8.00	8.01	8.00	8.00	8.00	8.00	8.00	8.00	8.00
Mg <sup>#</sup>	0.06	0.09	0.09	0.09	0.08	0.09	0.09	0.09	0.09	0.08	0.08	0.08	0.09	0.09	0.09	0.07
Almandine	84.07	81.08	81.50	79.79	80.54	79.81	79.22	77.09	77.73	77.38	79.26	79.22	79.44	80.15	80.98	81.93
Andradite	0.00	0.00	0.00	0.00	0.00	0.00	0.00	0.00	0.00	0.00	0.00	0.00	0.00	0.00	0.00	0.00
Grossular	0.47	1.30	1.29	1.25	1.22	1.28	0.95	1.13	1.22	1.04	1.37	1.31	1.33	1.18	1.25	0.46
Pyrope	5.24	7.71	8.20	7.78	7.29	7.68	7.46	7.93	7.03	7.20	6.69	7.60	8.15	7.78	7.78	6.57
Spessartine	10.19	9.87	8.88	11.18	10.92	11.23	12.33	13.85	14.02	12.67	11.87	11.05	10.77	10.00	10.97	
Uvarovite	0.03	0.03	0.13	0.00	0.03	0.00	0.03	0.00	0.00	0.13	0.03	0.03	0.13	0.00	0.00	0.06

Table 8. Representative microprobe data (rim to core to rim) of garnet (sample DH-3-grain 548) from Dehnow mica schist and the calculated structural formula based on 12 oxygen atoms.

Sample no.	673	674	679	680	681	682	683	684	685	688	689	690	692	693	694	696	697	698	700	702	703	705	706	707	708	709		
SiO <sub>2</sub>	97.24	34.01	36.00	37.21	37.19	36.87	37.05	37.30	37.28	37.13	36.47	36.82	36.81	37.08	36.95	37.39	37.18	37.04	37.33	37.39	37.50	37.09	37.11	37.09	31.78	50.40		
TiO <sub>2</sub>	0.04	2.21	0.07	0.06	0.08	0.11	0.10	0.14	0.13	0.21	0.24	0.16	0.15	0.17	0.13	0.15	0.18	0.11	0.14	0.21	0.20	0.11	0.04	1.26	0.05			
Al <sub>2</sub> O <sub>3</sub>	0.52	19.72	21.47	21.27	21.56	21.49	21.36	21.36	21.42	21.20	21.07	21.32	21.41	21.42	21.04	21.19	21.38	21.31	21.35	21.24	20.98	21.13	21.38	21.08	22.34	49.48		
Cr <sub>2</sub> O <sub>3</sub>	0.00	0.04	0.06	0.01	0.02	0.03	0.02	0.00	0.04	0.01	0.03	0.01	0.01	0.01	0.00	0.03	0.01	0.01	0.00	0.02	0.03	0.00	0.00	0.02	0.00	0.03		
FeO	0.41	23.57	36.35	36.86	36.79	37.05	37.25	37.00	36.46	36.10	36.31	36.15	36.07	35.80	35.70	36.15	35.94	35.92	35.84	35.64	35.65	36.47	36.64	36.49	21.09	0.43		
MnO	0.01	0.06	4.19	2.98	2.96	2.68	2.50	2.68	3.14	3.73	3.46	3.36	3.30	3.80	4.16	3.84	3.73	3.71	3.68	3.86	4.09	2.88	2.91	4.15	0.09	0.01		
MgO	0.06	5.97	1.22	1.96	1.99	2.06	1.95	1.95	2.02	1.91	1.92	1.94	2.00	1.77	1.32	1.82	1.89	1.93	1.87	1.75	2.07	2.01	1.31	7.07	0.01			
CaO	0.00	0.11	0.19	0.47	0.41	0.43	0.42	0.44	0.43	0.43	0.44	0.44	0.44	0.42	0.42	0.46	0.47	0.43	0.42	0.47	0.41	0.45	0.44	0.19	0.47	0.03		
Na <sub>2</sub> O	0.00	0.32	0.04	0.04	0.00	0.00	0.04	0.01	0.01	0.04	0.01	0.01	0.01	0.03	0.00	0.04	0.03	0.03	0.03	0.03	0.01	0.06	0.03	0.03	0.19	0.05		
K <sub>2</sub> O	0.09	7.50	0.07	0.03	0.00	0.01	0.01	0.00	0.00	0.00	0.02	0.00	0.01	0.00	0.00	0.00	0.00	0.01	0.00	0.01	0.00	0.00	0.00	0.00	2.41	0.04		
Sum	98.39	93.52	99.65	100.88	101.01	100.73	100.71	100.88	100.93	100.78	99.93	100.25	100.20	100.50	99.73	101.04	100.81	100.64	100.61	100.62	100.70	100.34	100.65	100.38	86.73	100.53		
Si	5.50	2.96	2.95	2.98	2.97	2.98	2.99	2.99	2.97	2.97	2.98	2.97	2.98	3.00	3.00	2.98	3.00	3.00	3.00	3.02	2.99	3.00	3.02	2.98	3.00	2.76		
Al <sup>IV</sup>	0.00	0.04	0.05	0.01	0.02	0.03	0.02	0.01	0.01	0.01	0.03	0.02	0.01	0.03	0.02	0.03	0.02	0.01	0.01	0.01	0.01	0.00	0.01	0.00	0.01	0.02	0.24	
Al <sup>VI</sup>	0.04	2.03	2.02	2.01	2.02	2.01	2.02	2.02	2.00	2.01	1.99	2.01	2.02	2.02	2.01	2.01	2.02	2.01	2.01	2.02	2.01	2.02	2.01	2.02	2.02	2.14	3.47	
Ti	0.00	0.15	0.00	0.00	0.01	0.01	0.01	0.01	0.01	0.01	0.01	0.01	0.01	0.01	0.01	0.01	0.01	0.01	0.01	0.01	0.01	0.01	0.01	0.01	0.01	0.08	0.00	
Cr	0.00	0.00	0.00	0.00	0.00	0.00	0.00	0.00	0.00	0.00	0.00	0.00	0.00	0.00	0.00	0.00	0.00	0.00	0.00	0.00	0.00	0.00	0.00	0.00	0.00	0.00		
Fe <sup>3+</sup>	0.00	0.00	0.00	0.00	0.00	0.00	0.00	0.00	0.00	0.00	0.00	0.00	0.00	0.00	0.00	0.00	0.00	0.00	0.00	0.00	0.00	0.00	0.00	0.00	0.00	0.00		
Fe <sup>2+</sup>	0.94	1.95	2.53	2.50	2.52	2.54	2.52	2.52	2.48	2.46	2.49	2.48	2.46	2.47	2.47	2.46	2.47	2.45	2.45	2.45	2.45	2.45	2.45	2.45	2.45	2.51	1.67	
Mn	0.00	0.00	0.29	0.20	0.18	0.17	0.18	0.21	0.25	0.24	0.23	0.23	0.26	0.29	0.26	0.25	0.25	0.26	0.25	0.25	0.26	0.28	0.20	0.28	0.20	0.28	0.00	
Mg	0.01	0.78	0.15	0.23	0.24	0.25	0.23	0.23	0.24	0.23	0.24	0.23	0.24	0.21	0.16	0.22	0.23	0.23	0.22	0.22	0.21	0.25	0.24	0.16	0.92	0.00		
Ca	0.00	0.01	0.02	0.04	0.04	0.04	0.04	0.04	0.04	0.04	0.04	0.04	0.04	0.04	0.04	0.04	0.04	0.04	0.04	0.04	0.04	0.04	0.04	0.04	0.04	0.00		
Na	0.00	0.00	0.00	0.00	0.00	0.00	0.00	0.00	0.00	0.00	0.00	0.00	0.00	0.00	0.00	0.00	0.00	0.00	0.00	0.00	0.00	0.00	0.00	0.00	0.00	0.00		
K	0.00	0.00	0.00	0.00	0.00	0.00	0.00	0.00	0.00	0.00	0.00	0.00	0.00	0.00	0.00	0.00	0.00	0.00	0.00	0.00	0.00	0.00	0.00	0.00	0.00	0.00		
Sum	6.48	7.92	8.02	8.00	8.01	8.00	8.00	8.00	8.01	8.00	7.99	7.99	7.99	8.00	7.99	7.99	7.99	7.99	7.99	7.99	7.99	8.00	7.99	8.04	8.15			
Mg#	0.01	0.28	0.06	0.09	0.09	0.08	0.08	0.09	0.09	0.09	0.09	0.09	0.09	0.08	0.08	0.06	0.08	0.08	0.08	0.09	0.08	0.09	0.09	0.06	0.33	0.00		
Almandine	89.40	71.17	84.52	83.97	84.08	84.26	85.21	84.76	83.45	82.49	82.83	83.13	83.04	82.89	83.66	82.64	82.48	82.37	82.74	82.33	82.28	83.68	83.95	84.53	65.04	99.83		
Andradite	0.00	0.00	0.00	0.00	0.00	0.00	0.00	0.00	0.00	0.00	0.00	0.00	0.00	0.00	0.00	0.00	0.00	0.00	0.00	0.00	0.00	0.00	0.00	0.00	0.00	0.00		
Grossular	0.00	0.24	0.36	1.33	1.16	1.13	1.27	1.11	1.15	1.26	1.20	1.22	1.18	1.23	1.13	1.34	1.26	1.14	1.11	1.31	1.22	0.56	1.40	0.00				
Pyrope	10.06	28.28	5.07	7.87	7.99	8.33	7.84	8.13	7.72	7.83	7.84	8.10	7.15	7.35	7.63	7.77	7.55	7.57	7.08	8.38	8.12	5.33	33.14	0.03				
Spessartine	0.54	0.17	9.85	6.81	6.75	6.16	5.72	6.12	7.16	8.55	8.04	7.73	7.59	8.74	9.70	8.80	8.55	8.51	8.45	8.88	9.43	6.63	9.59	0.24	0.04			
Uvarovite	0.00	0.15	0.21	0.02	0.05	0.10	0.07	0.07	0.14	0.09	0.10	0.05	0.14	0.09	0.10	0.01	0.03	0.00	0.00	0.08	0.10	0.10	0.01	0.06	0.00	0.17	0.10	

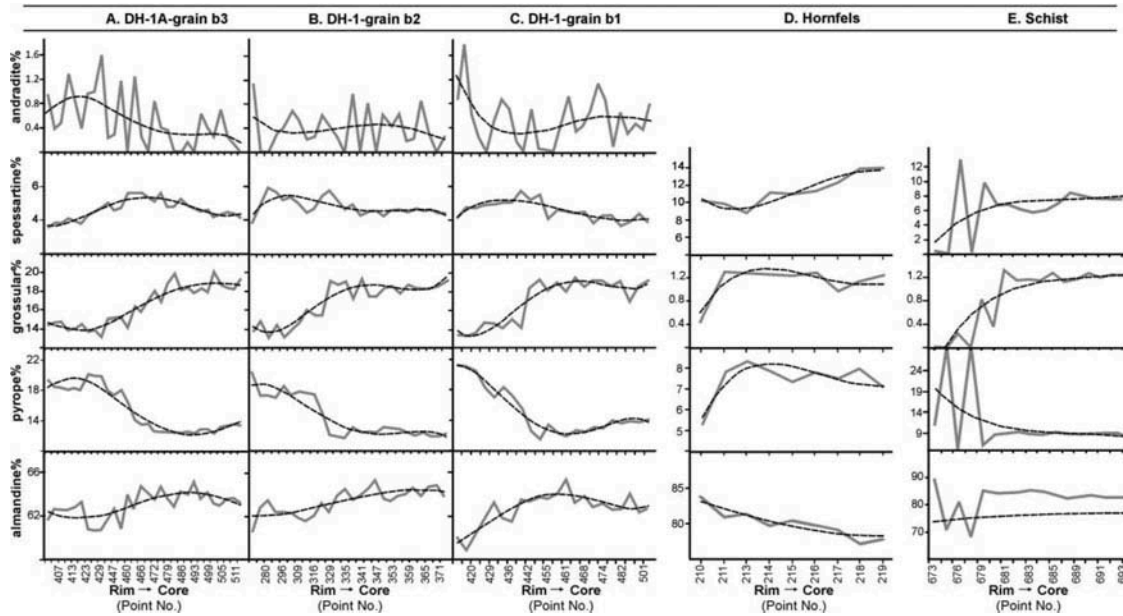


Figure 5. Zoning profiles of representative garnet megacrysts from the Dehnow DTG pluton (including sample DH1-grain 1, sample DH1-grain 2, sample DH1A-grain b3), hornfels (sample VR860824-5), and mica schist (sample DH-860824-2). The polynomial trend lines are drawn to clarify the complex zoning patterns. The profile scale is ~10 mm and 1 mm for the garnets from the Dehnow DTG pluton and the surrounding metapelitic rocks. The X-axis refers to point numbers in Tables 6 to 8 and analytical lines of Figure 3B, D, F.

In contrast to the DTG pluton, garnet in the metamorphic rocks has erratic zoning profiles. The best zoning patterns, based on 3rd degree polynomial regression trend lines (Figure 5D, E), indicate that the garnet from hornfels is characterized by a negative Mn–Fe correlation with core-to-rim increase in Fe and decrease in Mn, Ca, and Mg. The garnet from mica schist has a negative Mn–Mg correlation, with core-to-rim increase in Mg and decrease in Mn and Fe (Figure 5). In the schist and hornfels, the core-to-rim decrease in Mn in the garnet porphyroblasts is due to temperature reduction in the host metamorphic rock.

Volume diffusion in high-grade garnet usually obliterates growth zoning and would tend to homogenize its composition (Tuccillo *et al.* 1990). However, diffusion is unlikely to have significantly affected the composition of the different garnets in this study because compositional zoning is common in the garnets of the DTG pluton, hornfels, and mica schist (Figure 5).

Based on temperature and melt viscosity, Hawkesworth *et al.* (2000) suggested that crystal growth rates in magmatic systems are fast ( $10^{-10}$ – $10^{-11}$  cm/s). This means that a 10 mm crystal would take  $10^2$ – $10^3$  years to grow, compatible with the duration of magmatic events. The timescale of magmatic processes in granite genesis, from melting to crystallization, rarely exceeds  $10^5$  years (Villaros *et al.* 2009 and references therein). The experiments of Korolyuk and Lepegin (2008) show that the diffusion coefficients ( $D_c$ ) of Ca, Mg, Fe, and Mn are

in the order  $D_{\text{Mn}} > D_{\text{Fe}} > D_{\text{Mg}} > D_{\text{Ca}}$ . Diffusion coefficients are pressure-independent, but temperature-dependent. Korolyuk and Lepegin (2008) indicate that at 500 °C, the homogenization of a garnet grain of 1 mm radius, with an extremely inhomogeneous distribution of major components, will take  $1 \times 10^9$ ,  $1.5 \times 10^9$ ,  $2 \times 10^9$ , and  $3 \times 10^9$  years for Mn, Fe, Mg, and Ca, respectively. At a higher temperature (650°C), the process will take  $1 \times 10^7$ ,  $5 \times 10^7$ ,  $1 \times 10^9$ , and  $1.5 \times 10^9$  years, respectively. However, the actual  $D_c$  of elements in natural garnet must be higher than these experimental values (Korolyuk and Lepegin 2008). Considering the possible cooling rate and magmatic time scale of the DTG pluton (< $10^7$  years), the large size of garnet (~10–20 mm), and Ca and Mg zoning, it seems that diffusion had no significant effects on garnet composition. For example, the Fe content (Fe has a high  $D_c$ ) is variable and is higher in hornfels garnet than in the DTG pluton and mica schist. If significant Fe diffusion had occurred, the Fe content of garnet in the hornfels would have reached the average Fe value in the DTG pluton and mica schist.

#### *fO<sub>2</sub>* and P-T history of garnet crystallization

An increase in the oxygen fugacity in the melt favours the incorporation of  $\text{Fe}^{3+}$  over  $\text{Al}^{3+}$  into octahedral sites in the garnet (Scheibner *et al.* 2007). Thus, higher andradite content in the rim of magmatic garnets reflects the higher oxygen fugacity in the host melt; in contrast, the absence

Table 9. Representative whole-rock XRF data of the Dehnow DTG pluton (diorite, tonalite, granodiorite) hornfels and mica schist. Total iron concentration is expressed as  $\text{Fe}_2\text{O}_3$ .

Rock type	Granodiorite				Tonalite				Diorite				Hornfels		Mica schist	
	Sample no.	TD4	GD2.2	GD1.1	GD2.1	GD1.2	TD1	TD3	DH-2011-1*	DH-2011-4*	Sch-D	DH-2011-2*	DH-2011-3*			
SiO <sub>2</sub>	65.37	65.98	66.25	66.50	66.60	63.12	64.18	58.02	56.91	52.28	62.88	59.91				
Al <sub>2</sub> O <sub>3</sub>	13.21	14.74	15.02	14.54	14.32	15.18	14.25	18.07	21.57	20.56	18.64	19.31				
Fe <sub>2</sub> O <sub>3</sub> (total)	7.37	5.21	4.68	5.09	4.98	7.07	7.07	7.51	10.04	15.57	9.09	11.58				
FeO	5.28	3.34	2.86	3.23	3.13	5.01	5.01	5.41	7.68	12.66	6.83	9.07				
Fe <sub>2</sub> O <sub>3</sub>	2.09	1.87	1.82	1.86	1.85	2.06	2.06	2.10	2.36	2.91	2.26	2.51				
MnO	0.14	0.11	0.10	0.10	0.12	0.13	0.13	0.15	0.14	0.14	0.16	0.21				
MgO	2.56	2.28	2.12	2.28	2.29	2.14	2.14	2.52	2.31	1.59	1.69	1.58				
CaO	4.61	4.62	4.81	4.52	4.80	5.86	5.29	6.50	6.32	0.32	0.59	0.36				
Na <sub>2</sub> O	1.62	2.22	2.29	2.09	2.03	1.85	1.71	2.53	1.19	0.66	0.99	0.59				
K <sub>2</sub> O	2.93	2.63	2.65	2.71	2.62	2.35	2.54	2.63	2.20	2.58	2.42	1.74				
TiO <sub>2</sub>	0.72	0.50	0.43	0.49	0.46	0.69	0.69	0.77	0.86	0.90	1.06	0.95				
P <sub>2</sub> O <sub>5</sub>	0.21	0.16	0.16	0.14	0.16	0.23	0.23	0.21	0.07	0.09	0.13	0.09				
LOI	1.15	0.96	1.25	1.08	1.09	1.22	1.19	1.37	1.37	3.66	4.09	3.37	3.11			
Total	99.9	99.4	99.8	99.5	99.8	99.8	99.8	100.1	98.6	99.2	100.7	99.6				
K <sub>2</sub> O+Na <sub>2</sub> O	4.55	4.85	4.94	4.80	4.65	4.20	4.25	5.16	3.39	3.24	3.41	2.33				
Mg#	0.33	0.41	0.43	0.41	0.42	0.30	0.33	0.30	0.17	0.12	0.19	0.16				
A/CNK	0.9	1.0	1.0	1.0	1.0	0.9	0.9	1.0	4.4	4.2	3.8	5.5				

Note: \* Analysed at ActLabs.

Table 10.  $\delta^{18}\text{O}$  values of garnet, quartz, and biotite grains from the Dehnow DTG pluton, mica schist, and hornfels.

Sample no.	Rock type	$\delta^{18}\text{O}_{\text{garnet}}$	$\delta^{18}\text{O}_{\text{quartz}}$	$\delta^{18}\text{O}_{\text{biotite}}$	$\delta^{18}\text{O}_{\text{whole rock}}$	$\Delta_{\text{quartz-garnet}}$	$\Delta_{\text{quartz-biotite}}$	$T_{\Delta\text{quartz-garnet}} (\text{°C})$	$T_{\Delta\text{quartz-biotite}} (\text{°C})$
DH-2011-1-1	Granitoid	8.73	11.80	7.01	n.a	3.07	4.79	666	398
DH-2011-1-2	Granitoid	8.60	11.51	n.a	n.a	2.91	-	692	-
DH-2011-1-3	Granitoid	8.64	n.a	n.a	n.a	-	-	-	-
DH-G2013-2	Granitoid	8.33	n.a	n.a	n.a	-	-	-	-
DH-G2013-3	Granitoid	8.51	14.73	n.a	n.a	6.22	-	-	387
DH-G2013-4	Granitoid	8.45	n.a	n.a	n.a	-	-	-	-
DH-G2013-5	Granitoid	8.54	12.20	n.a	n.a	3.66	-	-	586
DH-G2013-H1	Hornfels	13.12	n.a	n.a	n.a	-	-	-	-
DH-G2013-Sch1	Mica schist	12.54	n.a	n.a	n.a	-	-	-	-
DH-G2013 Sch2	Mica schist	13.81	n.a	n.a	n.a	-	-	-	-
DH-2011-2	Mica schist	12.74	n.a	n.a	n.a	16.0	-	-	-
DH-2011-3	Mica schist	12.98	n.a	n.a	n.a	15.9	-	-	-
DH-2011-4	Mica schist	12.92	n.a	n.a	n.a	14.8	-	-	-

Note: n.a.: not analysed.

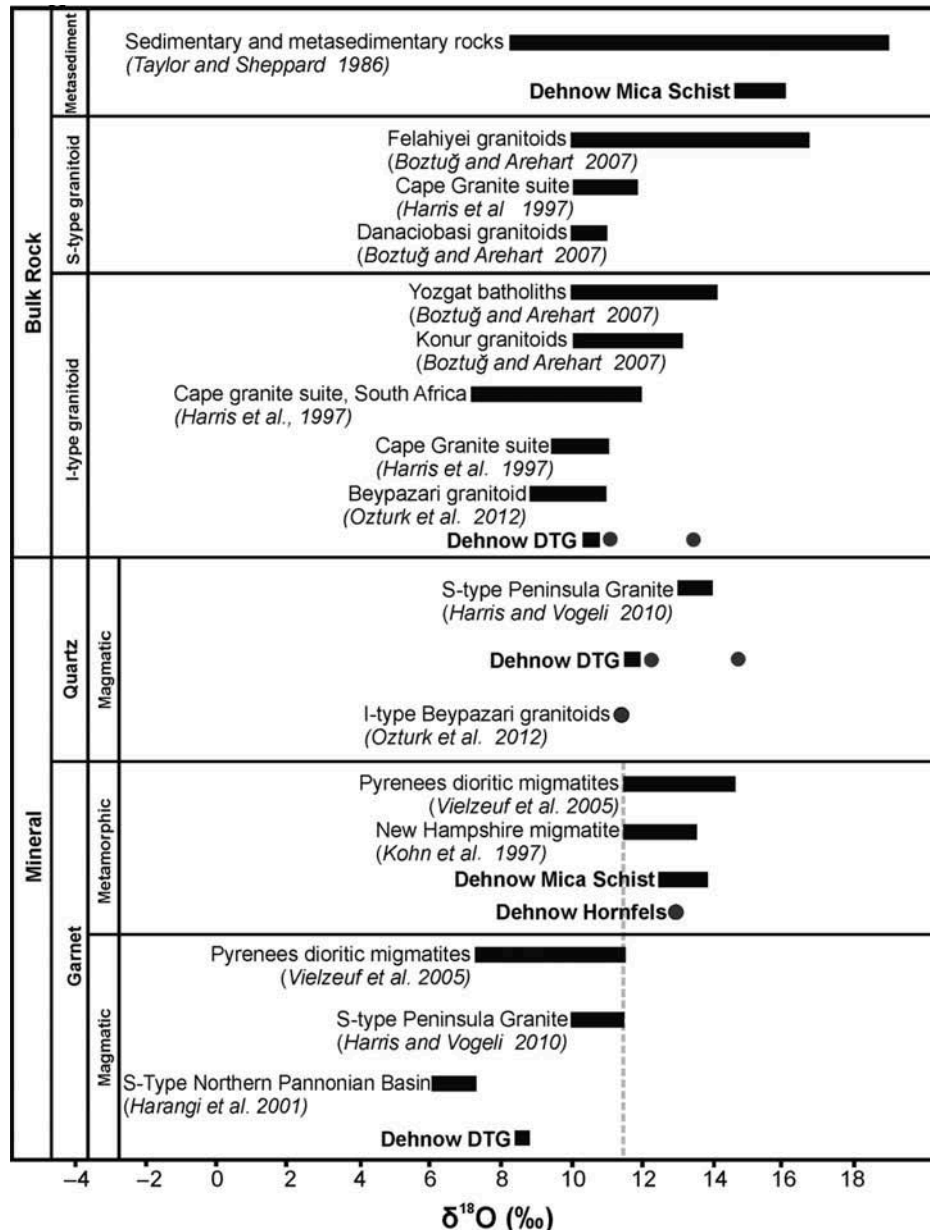


Figure 6. Comparison of  $\delta^{18}\text{O}$  values of bulk rock quartz and garnet from the Dehnow DTG pluton and surrounding metapelitic rocks with available data from sedimentary and igneous rocks in general, and for other examples of magmatic and metamorphic garnet and quartz.

of an andradite component in the garnet of metapelitic rocks indicates a reducing metamorphic environment. In addition, epidote stability is limited to high oxygen fugacities, equal to or above the haematite-magnetite (HM) oxygen buffer (Poli and Schmidt 2004).  $X_{\text{ep}}$  of the epidote inclusions shows a decrease from garnet core to rim. Several geobarometers and geothermometers have been proposed to estimate the P-T conditions of granitoid batholith formation (e.g. Holland and Blundy 1994; Anderson 1996; Holdaway et al. 1997). Because garnets in the DTG pluton contain inclusions of plagioclase, hornblende, and biotite, the Al-in-hornblende barometer (Schmidt 1992),

amphibole-plagioclase thermometer (Blundy and Holland 1990), garnet-biotite thermometer (Holdaway 2000), and garnet-biotite-plagioclase-quartz barometer of Wu et al. (2004) can provide direct constraint on the crystallization pressure of garnet. Al-in-hornblende geobarometry and amphibole-plagioclase thermometry, which are preferred for metaluminous granites (Anderson et al. 2008), revealed pressures of ~6.4 kbar and temperatures of ~708°C for the DTG pluton. The garnet-biotite thermometer and garnet-biotite-plagioclase-quartz barometer, which are recommended for peraluminous granites (Anderson et al. 2008), yielded a temperature of ~790°C

Table 11. Summary of case studies investigating the origin of garnet in igneous rocks. 'I' denotes magmatic garnet phenocrysts and 'M' metamorphic garnet xenocrysts (n.a., not available; n.z., not zoned).

Author	Rock type	Garnet type	Rim	Core	CaO (wt%)	MnO (wt%)	Origin
Green and Ringwood (1968)	Rhyodacite and Granodiorite	Alm-rich	Alm-Sps	PPr	0.69	1.9	I
Brousse <i>et al.</i> (1972)	Andesite (Samples A and B)	Alm-rich	Alm-Sps-Grs	PPr	2.24	10.05	I
Brousse <i>et al.</i> (1972)	Rhyolite (Sample C)	Alm-rich	Alm-PPr	Sps-Grs	2.24	10.05	I
Fittou (1972)	Andesite and Dacite	Alm-rich	PPr	Alm	1.26	2.16	I
Vennemann and Meyer (1979)	Diorite-Granodiorite	Alm-rich	Alm-Sps	PPr-Grs	1.00>	13.00<	I
Miller and Stoddard (1981)	Granite, Aplite and Pegmatite	SpS-rich	Alm	Sps	0.46	0.68	I
Plank (1987)	Granite	PPr (Alm)-rich	Alm	PPr	1.33>	2.00>	I
Hanner and Moyes (1982)	Andesite ~ Rhyolite (S-type)	Alm-rich	Alm-PPr	Grs	3.50	1.80	I
du Bray (1988)	Alm (SpS)-rich	SpS	Alm	0.15	1.1	n.a.	I
Dobbe (1992)	SpS-rich	Alm-PPr	SpS	n.a.	n.a.	n.a.	I
Jung <i>et al.</i> (2001)	Granite	Alm-rich	SpS-Grs	PPr	2.17>	7.99>	I
Harangi <i>et al.</i> (2001)	Rhyodacite (type 1A)	Alm-rich	Grs	PPr	4.5-5.4	1.7-2.3	I
Harangi <i>et al.</i> (2001)	Dacite (type 1B)	Alm-rich	PPr-Grs	Alm-Sps	4.9-8.1	0.8-3.0	I
Harangi <i>et al.</i> (2001)	Andesite (type 2)	Alm-rich	PPr	Grs-Sps	4.6-6.0	1.8-3.0	I
Harangi <i>et al.</i> (2001)	Andesite, Dacite (type 3composite – core)	Alm-rich	n.a.	n.a.	0.8-1.6	0.7-7.1	M
Harangi <i>et al.</i> (2001)	Andesite, Dacite (type 3composite – rim)	Alm-rich	n.a.	n.a.	4.2-8.1	0.8-2.7	I
Harangi <i>et al.</i> (2001)	Xenolith in Andesite (type 4)	Alm-rich	PPr-Grs	Alm-Sps	0.8-2.7	3.3-10.9	M
Aydar and Gourgaud (2002)	Basalt	Alm (PPr)-rich	n.a.	n.a.	5.97	1.00>	I
Kawabata and Takafuji (2005) (I)	Dacite	Alm-rich	PPr-Grs	Alm-Sps	1.16-2.99	5.06-6.48	I
Kawabata and Takafuji (2005) (M)	Dacite	Alm-rich	PPr	SpS	0.24-6.31	1.30-7.23	M
Rene and Stelling (2007)	Granite (Garnet group I)	Alm (SpS)-rich	SpS	PPr	0.9>	5.56>	I
Dahlquist <i>et al.</i> (2007)	Granite	Alm-rich	Unzoned	PPr-Alm	2.00>	28.00>	I
Patranabis-Deb <i>et al.</i> (2009)	Rhyolitic tuff	Alm-rich	PPr-Sps	Alm	0.07-2.64	0.06-0.80	I
Yuan <i>et al.</i> (2008)	Tonalitic porphyry	Alm-rich	n.z.	n.z.	5.27	11.41	I
Mirnejad <i>et al.</i> (2008)	Rhyolite	Alm-rich	Alm	n.z.	3.05	5.66	I
Haris and Vogeli (2010)	Granite	Alm-rich	Alm	PPr	n.a.	n.a.	I
Zhang <i>et al.</i> (2012)	Granite	SpS (Alm)-rich	SpS	Grs	1.09-5.84	24.21-27.44	I
Bach <i>et al.</i> (2012)	Andesite (Sample 1A)	Alm (PPr)-rich	PPr	Alm-Grs	7.98-6.75	0.68-0.75	I
Bach <i>et al.</i> (2012)	Andesite (Sample 1B)	PPr (Alm)-rich	PPr	Grs	7.89-9.22	0.85-0.86	I
Bach <i>et al.</i> (2012)	Andesite (Sample 1C)	Alm (PPr)-rich	Grs-PPr	Alm	8.20-9.36	1.03-1.70	I
Bach <i>et al.</i> (2012)	Andesite (Sample 1D)	Alm-rich	PPr	1.6-9	0.84-1.51	I	
This Study	Granitoid	Alm (Grs>PPr)-rich	PPr	Alm-Grs	4.7-7.1	1.6-4.3	I

and 8.4 kbar. These results suggest a crystallization depth of ~22–30 km (the upper lithosphere) (Samadi 2009). Abbott and Clarke (1979); Miller and Stoddard (1981), and Abbott (1981a, b) discussed how garnet could crystallize at the expense of biotite in MnO- and Al<sub>2</sub>O<sub>3</sub>-rich evolved magma. Based on the paragenesis of biotite + hornblende → biotite + hornblende + garnet (consistent with the petrography), the AFM of Abbott (1981b) indicates temperatures greater than ~800°C, and  $a_{\text{H}_2\text{O}} \ll 1$  (equilibrium z-z line in Figure 3 of Abbott 1981b). Day *et al.* (1992) demonstrated that the assemblage garnet + plagioclase + amphibole + quartz is stable at 10 kbar and 800–850°C in a garnet-bearing andesite from New Zealand. Green (1992) demonstrated that a mineral assemblage of garnet + plagioclase + amphibole in dacitic magma with 5% H<sub>2</sub>O would be stable at 8–13 kbar and 820–920°C. Many other researchers (e.g. Green and Ringwood 1968; Clemens and Wall 1988; Conrad *et al.* 1988; Spear and Cheney 1989; Vielzeuf and Montel 1994; Harangi *et al.* 2001; Kawabata and Takafuji 2005) have shown that garnet with high CaO (>4 wt.%) and low MnO (<4 wt. %), together with Ca-rich plagioclase and amphibole, is indicative of high pressures (7–12 kbar) and temperatures (800–950°C). CaO and MnO contents (core to rim) of garnet in the DTG pluton are ~7.44–4.91 wt.% and ~1.94–2.84 wt.%, respectively.

These results confirm that garnet crystallized at a high P-T condition and garnet growth reached 7–12 kbar and 800–950°C in the lower crust. The high Ca and low Mn in the garnet core indicate higher P-T conditions for the core relative to the rim. On the other hand, the average  $X_{\text{ep}}$  of epidote inclusions in the garnets (~0.32) and epidote in the matrix (~0.24), together with the grossular-andradite solid solution ( $X_{\text{adr}} = 100 \times \text{Fe}^{3+}/(\text{Al} + \text{Fe}^{3+} + \text{Cr}^{3+}) \sim <0.1\%$ ) at  $f\text{O}_2$  fixed by the HM buffer (by Heuss-Aßbichler and Fehr 1997) (Figure 7), indicate that garnet-epidote equilibrium temperatures are higher than 650°C, and even close to 800 °C (Figure 7).

Regarding oxygen diffusion, the  $\Delta_{\text{quartz-garnet}}$  values of 6.2, 3.6, 3.0, and 2.9‰ for the DTG pluton indicate the closure temperatures of 387, 586, 666, and 692°C, calculated using the fractionation equation of Valley *et al.* (2003), in which  $\Delta_{\text{quartz-almandine}} = 2.71 \times 10^6/T^2$ , and a  $\Delta_{\text{quartz-biotite}}$  value of 4.5‰ for the DTG pluton corresponds to the closure temperature of 398 °C for oxygen diffusion (using the fractionation equation of Chacko *et al.* (2001), in which  $\Delta_{\text{quartz-biotite}} = 2.16 \times 10^6/T^2$ ) (Table 10). Lower oxygen closure temperature for quartz-biotite and biotite inclusions in the garnet indicates that biotite continues to diffuse oxygen for a longer period after oxygen diffusion has ceased in garnet.

Therefore, crystallization conditions of the garnet and the ascending host melt were at ~708–800°C and 6.4–12 kbar (for the hornblende-plagioclase, garnet-biotite, garnet-biotite-plagioclase-quartz, and garnet-epidote equilibria).

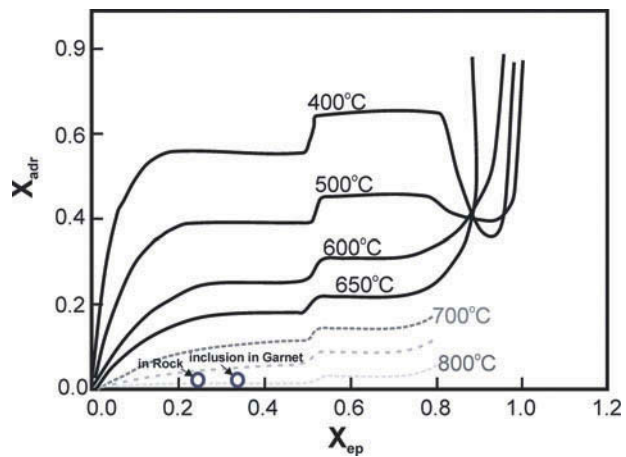


Figure 7. Partitioning of Al and Fe<sup>3+</sup> between the grossular-andradite solid solution and the clinozoisite-epidote solid solution at  $f\text{O}_2$  fixed by the HM buffer (Poli and Schmidt 2004 and references therein, with some modifications). The higher temperatures of 700°C and 800°C are estimated based on the extrapolated dashed lines (adr = andradite; ep = epidote).

The garnet megacrysts recorded oxygen diffusion temperatures of ~692–387°C.

#### Magmatic origin of garnet in Dehnow DTG pluton

Scallion *et al.* (2011) considered assimilation and contamination by host rock as the most important processes for garnet origin in the granitoid pluton. Petrographic and geochemical reasons indicate that the garnets in the DTG pluton did not originate from the adjacent metamorphic rocks, nor was it an antecrust after an antelith (based on Bach *et al.* 2012). The term antecrust is used for crystals that belong in the magmatic system that produced the host but are not directly a consequence of the crystallization of the host, and the term antelith is used for enclaves that are considered to be part of the petrogenetic process that produced their hosts and xenolith for enclaves that are clearly foreign to their host. In addition, the lack of garnet-bearing xenoliths in the DTG pluton and the absence of sillimanite (fibrolite) and cordierite inclusions in the garnet megacrysts of the DTG pluton indicate that the DTG pluton and garnet genesis is not related to the adjacent metapelitic rocks. Moreover, the large size (~10–20 mm) of garnet crystals in the DTG pluton would be difficult to reconcile with the small garnet grains (~2 mm) found in the metamorphic rocks. The lack of reaction rims in the euhedral to subhedral garnet in the DTG pluton is consistent with the garnet growth under equilibrium conditions. The compositional zoning patterns of the DTG garnet also differ from those of the metamorphic garnet in the surrounding hornfels and mica schist. The distinctly different composition (from rim to core) of the garnet megacrysts in the DTG pluton relative to the composition

of the garnet grains in the schist suggests different conditions of formation. Differences in  $\delta^{18}\text{O}$  values of DTG garnet megacrysts and garnet grains in the adjacent mica schist indicate that garnet megacrysts cannot be a refractory restite phase that survived partial melting of the surrounding metamorphic rocks or partial melting in the source region. The  $\delta^{18}\text{O}$  value of garnets in the DTG pluton (8.3–8.7‰) is lower than  $\delta^{18}\text{O}$  values in the metamorphic rocks (12.5–13.1‰). Generally, magmatic garnet has lower  $\delta^{18}\text{O}$  values than garnet in pelitic metamorphic rocks, because the protoliths of the latter are rich in low-temperature minerals such as clays (e.g. Sharp 2006). As shown in Figure 6, the  $\delta^{18}\text{O}$  values of magmatic garnet

from the Northern Pannonian Basin (Harangi *et al.* 2001) are 6.1–7.2‰. Harris and Vogeli (2010) reported  $\delta^{18}\text{O}$  values of 10.0–11.4‰ for magmatic garnet and 13.2–14.0‰ for quartz in S-type granites, formed by partial melting of metapelitic rocks. Vielzeuf *et al.* (2005) reported  $\delta^{18}\text{O}$  values of 7.3–11.6‰ for the magmatic rim of composite garnets in dioritic migmatites.  $\delta^{18}\text{O}$  values of 11.4–13.4‰ (Kohn *et al.* 1997) and 11.6–14.4‰ (Vielzeuf *et al.* 2005) were obtained for metamorphic garnets. The  $\delta^{18}\text{O}$  values for garnet from the DTG pluton are comparable with magmatic garnet from other studies (Figure 6). In addition, the co-variation in garnet and quartz  $\delta^{18}\text{O}$  values for the DTG pluton is comparable to the other

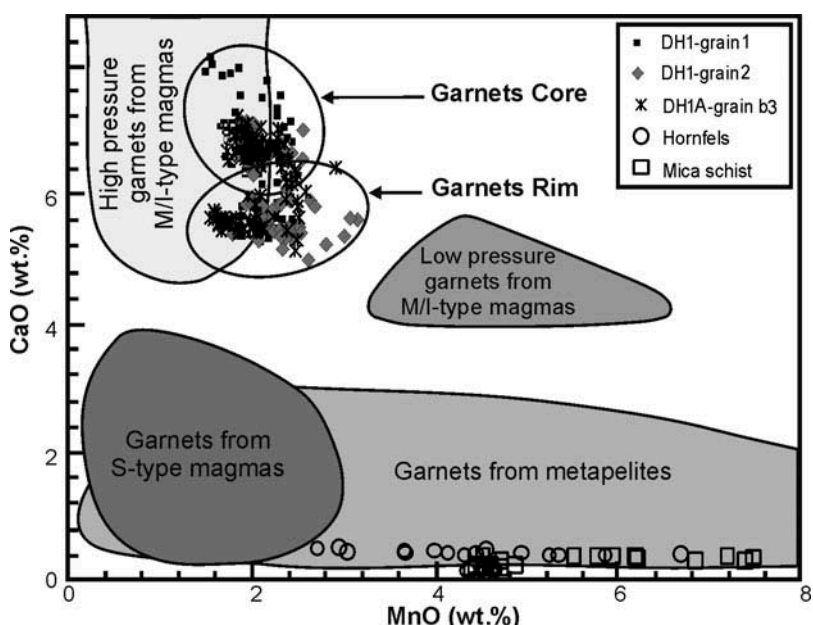


Figure 8. Plot of CaO versus MnO (after Harangi *et al.* 2001). Core and rim composition of garnet in the DTG pluton is compared. Garnet from DTG is ‘high P-T garnet from I-type magma’. Garnet of mica schist and hornfels is correlated with garnet from ‘metapelitic rocks’.

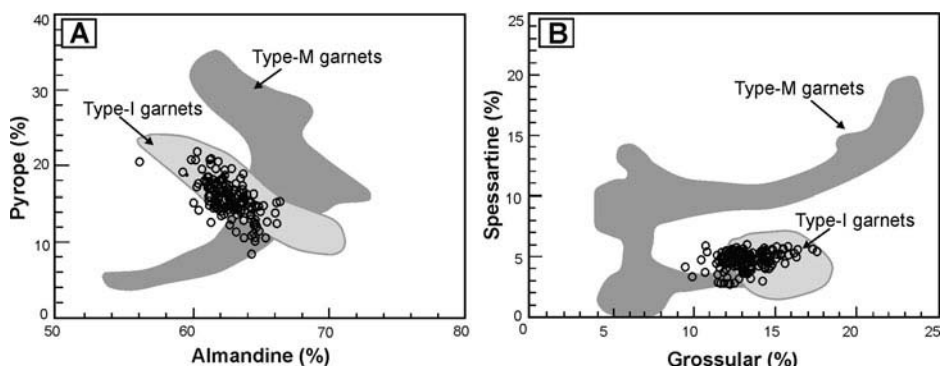


Figure 9. Garnet of the Dechnow DTG pluton (open circles) compared to the composition of M-type (metamorphic xenocrysts) and I-type (magmatic phenocrysts) garnet of Setouchi volcanic belt (Japan) (after Kawabata and Takafuji 2005).

examples of magmatic garnet (e.g. Cape Granite Suite, West Cape, Harris and Vogeli 2010; Sierra Nevada, USA, Lackey *et al.* 2008).

The Fe–Mg distribution between garnet and biotite ( $(\text{Mg}/\text{Fe})^{\text{Grt}}/(\text{Mg}/\text{Fe})^{\text{Bt}}$ ) for the DTG pluton and mica schist (0.36 and 0.15, respectively) is comparable to the corresponding values obtained for igneous (>0.24) and metamorphic rocks (<0.20) studied by Lyons and Morse (1970) and Harangi *et al.* (2001). The higher  $\text{Mg}^{\#}_{\text{garnet/biotite}}$  of the DTG pluton (~0.43) in comparison with hornfels (~0.24) and mica schists (~0.32), and the higher average  $\text{Mg}^{\#}_{\text{garnet/whole rock}}$  of the DTG pluton (~0.31) than mica schists (~0.161) can discriminate these magmatic and metamorphic garnets.

According to Evans and Vance (1987), the low  $\text{TiO}_2$  of epidote (<0.2 wt.%) in the cores of garnets (~0.02 wt.%) and the matrix (~0.12 wt.%) is consistent with a magmatic origin for garnets, whereas the epidotes in the rim fractures of garnet have higher  $\text{TiO}_2$  (~0.36 wt.%). Therefore the similar composition of magmatic amphibole, feldspar, and epidote in the groundmass with inclusions of the same minerals in the garnet megacrysts is consistent with a magmatic origin for the garnet as well as the magmatic nature of these inclusions.

Garnets found in metaluminous subduction-related hosts are characterized by higher  $\text{CaO}$  content (>4 wt.%) than that associated with peraluminous compositions (Bach *et al.* 2012). On the  $\text{MnO}$  versus  $\text{CaO}$  diagram (Harangi *et al.* 2001), the garnet plots in the high-pressure magmatic field for I/M-type mantle magmas, characterized by  $\text{CaO} > 4$  wt.% and  $\text{MnO} < 4$  wt.% (Figure 8). This diagram (Figure 8) also shows the identical chemical composition of garnet cores and rims, in contrast to the ‘composite garnet’ crystals described by Harangi *et al.* (2001). The ‘composite garnet’ crystals have light-coloured xenocrystic cores (reputedly derived from adjacent metapelitic rocks) with a magmatic overgrowth (e.g. Harangi *et al.* 2001; Vielzeuf *et al.* 2005). Kawabata and Takafuji (2005) divided the garnets from the peraluminous Setouchi volcanic rocks (Kawabata and Shuto 2005) into I and M types on the basis of petrography and chemistry. However, considering the metaluminous nature of the DTG pluton, our garnet samples show a strong affinity with the I-type (igneous) garnet phenocrysts and are distinctly different from the M-type (metamorphic) garnet (Figure 9A, B).

## Conclusions

The Dehnow garnet-bearing DTG intruded the remnants of the Palaeo-Tethys sequence in NE Iran. Dehnow DTG is an I-type calc-alkaline pluton, composed mainly of plagioclase, quartz, biotite, and accessory minerals which include alkali feldspar, amphibole, almandine-rich garnet, epidote, and ilmenite. Petrographic and geochemical evidence suggest that the DTG pluton formed from magmas

produced in lower crust, and that the garnet is magmatic. The character of the chemical zoning and the large size of DTG garnet indicate that subsolidus diffusion had negligible effects on growth.

The following criteria indicate that DTG garnets are not xenocrysts: (1) their large size (~10–20 mm), which distinguishes them from the small (~2 mm) garnets in the metamorphic rocks; (2) absence of garnet-bearing xenoliths in the DTG pluton and absence of sillimanite (fibrolite) and cordierite inclusions in garnet; (3) lack of evidence for assimilation at the margin of the DTG pluton; (4) the distinct composition of DTG garnet megacrysts relative to the composition of garnet in metapelitic rocks; and (5) the  $\delta^{18}\text{O}$  value of garnet in the DTG pluton (~8.3–8.7‰), which is lower than the  $\delta^{18}\text{O}$  of the garnet in the metamorphic rocks (~11.6–14.0‰).

Evidence for a magmatic origin of DTG garnet includes: (1) euhedral to subhedral form and absence of reaction rims; (2) Fe-rich composition of garnet, together with higher Mg and lower Ca at the rims; (3) amphibole, plagioclase, and biotite in Dehnow DTG pluton are similar in composition to inclusions of the same minerals in garnet; (4) epidote and amphibole inclusions in the garnet have a magmatic nature; and (5) the chemical composition of garnet which plots in the magmatic field on discrimination diagrams.

In contrast to the reduced, low- $f(\text{O}_2)$ , metamorphic environment of metapelitic rocks reflected in the low andradite content of metamorphic garnet, the higher andradite content in the rim of magmatic garnet reflects higher  $f(\text{O}_2)$  in the DTG melt. Garnet crystallization in DTG melt occurred at temperatures expected for intermediate to felsic melts of lower crust at ~800°C, and the closure temperatures of oxygen diffusion recorded in garnet megacrysts range from ~692 to 387°C.

## Acknowledgements

We thank the Institute for Research on Earth Evolution (Yokosuka, Japan), University of Cape Town, and the Department of Geosciences at Virginia Tech for financial supports and providing geochemical facilities. The authors express gratitude to the constructive reviews of Richard N. Abbott and Scott A. Whatman and one anonymous reviewer and the editorial handling of associated editor Bob Stern, which improved the original manuscript. This paper represents part of the first author’s PhD thesis research. The O-isotope work at the University of Cape Town was supported by a NRF grant to CH. We are grateful to Fayrooz Rawoot for assistance with the O-isotope analyses.

## References

- Abbott, R.N., Jr., 1981a, The role of manganese in the paragenesis of magmatic garnet: An example from the Old Woman Piute Range, California: A discussion: Journal of Geology, v. 89, no. 6, p. 767–769.

- Abbott, R.N., Jr., 1981b, AFM liquidus projection for granitic magmas, with Special reference to hornblende biotite and garnet: *Canadian Mineralogist*, v. 19, p. 103–110.
- Abbott, R.N., Jr., 1985, Muscovite bearing granites in the AFM liuidus projection: *Canadian Mineralogist*, v. 23, p. 553–561.
- Abbott, R.N., Jr., and Clarke, D.B., 1979, Hypothetical liquidus relationships in the subsystem  $\text{Al}_2\text{O}_3$ - $\text{FeO}$ - $\text{MgO}$  projected from quartz, alkali feldspar, and plagioclase for  $a(\text{H}_2\text{O}) < 1$ : *Canadian Mineralogist*, v. 17, p. 549–560.
- Alavi, M., 1991, Sedimentary and structural characteristics of the Paleo-Tethys remnants in northeastern Iran: *Bulletin of Geological Society of America*, v. 103, p. 983–992.
- Allan, B.D., and Clarke, D.B., 1981, Occurrence and origin of garnets in the south mountain batholith, Nova Scotia: *The Canadian Mineralogist*, v. 19, p. 19–24.
- Anderson, J.L., 1996, Status of thermobarometry in granitic batholiths: *Transactions of the Royal Society of Edinburgh: Earth Sciences*, v. 87, p. 125–138.
- Anderson, J.L., Barth, A.P., Wooden, J.L., and Mazdab, F., 2008, Thermometers and thermobarometers in granitic systems: *Reviews in Mineralogy and Geochemistry*, v. 69, p. 121–142.
- Aydar, E., and Gourgaud, A., 2002, Garnet-bearing basalts: an example from Mt. Hasan, Central Anatolia, Turkey: *Mineralogy and Petrology*, v. 75, p. 185–201.
- Bach, P., Smith, I.E.M., and Malpas, J.G., 2012, The origin of garnets in andesitic rocks from the Northland arc, New Zealand, and their implication for sub-arc processes: *Journal of Petrology*, v. 53, p. 1169–1195.
- Bindeman, I.N., 2008, Oxygen isotopes in mantle and crustal magmas as revealed by single crystal analysis, in Putirka, K. D., and Tepley, F.J., eds., *Minerals, inclusions and volcanic processes: Mineralogical Society of America and Geochemical Society, Reviews in Mineralogy and Geochemistry*, v. 69, p. 445–478.
- Blundy, J.D., and Holland, T.J.B., 1990, Calcic amphibole equilibria and a new amphibole-plagioclase geothermometer: *Contributions to Mineralogy and Petrology*, v. 104, p. 208–224.
- Boztuğ, D., and Arehart, G.B., 2007, Oxygen and sulfur isotope geochemistry revealing a significant crustal signature in the genesis of the post-collisional granitoids in central Anatolia, Turkey: *Journal of Asian Earth Sciences*, v. 30, p. 403–416.
- Brousse, R., Bizouard, H., and Salat, J., 1972, Grenats des andésites et des rhyolites de Slovaquie, origine des grenats dans les séries andésitiques: *Contributions to Mineralogy and Petrology*, v. 35, p. 201–213.
- Chacko, T., Cole, D.R., and Horita, J., 2001, Equilibrium oxygen, hydrogen, and carbon isotope fractionation factors applicable to geological systems, in Valley, J.W., and Cole, D.R., eds., *Stable isotope geochemistry: Mineralogical Society of America-Geochemical Society, Reviews in Mineralogy and Geochemistry*, v. 43, p. 1–81.
- Clarke, D.B., and Rottura, A., 1994, Garnet forming and garnet eliminating reactions in quartz diorite intrusion at Capo Vaticano, Calabria, Southern Italy: *The Canadian Mineralogist*, v. 32, p. 623–635.
- Clemens, J.D., and Wall, V.J., 1988, Controls on the mineralogy of S-type volcanic and plutonic rocks: *Lithos*, v. 21, p. 53–66.
- Conrad, W.K., Nicholls, L.A., and Wall, V.J., 1988, Water-saturated and unsaturated melting of metaluminous and peraluminous crustal compositions at 10 kb: evidence for the origin of silicic magmas in the Taupo Volcanic Zone, New Zealand and other occurrence: *Journal of Petrology*, v. 29, p. 765–803.
- Dahlquist, J.A., Galindo, C., Pankhurst, R.J., Rapela, C.W., and Alasino, P.H., 2007, Magmatic evolution of the Peñón Rosado granite: Petrogenesis of garnet-bearing granitoids: *Lithos*, v. 95, p. 177–207.
- Day, R.A., Green, T.H., and Smith, I.E.M., 1992, The origin and significance of garnet phenocrysts and garnet-bearing xenoliths in Miocene calc-alkaline volcanics from Northland, New Zealand: *Journal of Petrology*, v. 33, p. 125–161.
- Deer, W.A., Howie, R.A., and Zussman, J., 1992, An introduction to the rock forming minerals (second edition): London, Longman.
- Dobbe, R.T.M., 1992, Zoned manganiferous garnets of magmatic origin from the Southern Uplands of Scotland: *Mineralogical Magazine*, v. 56, p. 115–116.
- du Bray, E.A., 1988, Garnet compositions and their use as indicators of peraluminous granitoid petrogenesis-southeastern Arabian Shield: *Contributions to Mineralogy and Petrology*, v. 100, p. 205–212.
- Evans, B.W., and Vance, J.A., 1987, Epidote phenocrysts in dacitic dikes, Boulder country, Colorado: *Contributions to Mineralogy and Petrology*, v. 96, p. 178–185.
- Farquhar, J., Chacko, T., and Ellis, D.J., 1996, Preservation of oxygen isotope compositions in granulites from Northwestern Canada and Enderby Land, Antarctica: implications for high-temperature isotopic thermometry: *Contributions to Mineralogy and Petrology*, v. 125, p. 213–224.
- Fittion, J.G., 1972, The genetic significance of Almandine-Pyrope Phenocrysts in the Calc-Alkaline Borrowdale Volcanic Group, Northern England: *Contributions to Mineralogy and Petrology*, v. 36, p. 231–248.
- Fourie, D.S., and Harris, C., 2011, O-isotope study of the Bushveld Complex Granites and Granophyres: Constraints on source composition, and assimilation: *Journal of Petrology*, v. 152, p. 2221–2242.
- Green, T.H., 1992, Experimental phase equilibrium studies of garnet-bearing I-type volcanics and high-level intrusives from Northland, New Zealand: *Earth and Environmental Science Transactions*, v. 83, p. 429–438.
- Green, T.H., and Ringwood, A.E., 1968, Origin of garnet phenocrysts in calc-alkaline rocks: *Contributions to Mineralogy and Petrology*, v. 18, p. 163–174.
- Hamer, R.D., and Moyes, A.B., 1982, Composition and origin of garnet from the Antarctic Peninsula Volcanic Group of Trinity Peninsula: *Journal of Geological Society*, v. 139, p. 713–720.
- Hammarstrom, J.M., and Zen, E., 1986, Aluminum in hornblende: An empirical igneous geobarometer: *American Mineralogist*, v. 71, p. 1297–1313.
- Harangi, S.Z., Downes, H., Kósa, L., Szabó, C.S., Thirlwall, M.F., and Mason, P.R.D., 2001, Almandine garnet in calc-alkaline volcanic rocks of the Northern Pannonian Basin (Eastern-Central Europe), geochemistry, petrogenesis and geodynamic implications: *Journal of Petrology*, v. 42, p. 1813–1843.
- Harris, C., and Ashwal, L.D., 2002, The origin of low  $\delta^{18}\text{O}$  granites and related rocks from the Seychelles: *Contributions to Mineralogy and Petrology*, v. 143, p. 366–376.
- Harris, C., Faure, K., Diamond, R.E., and Scheepers, R., 1997, Oxygen and hydrogen isotope geochemistry of S and I-type granitoids: The Cape Granite suite, South Africa: *Chemical Geology*, v. 143, p. 95–114.
- Harris, C., and Vogeli, J., 2010, Oxygen isotope composition of garnet in the Peninsula Granite, Cape Granite Suite, South Africa: Constraints on melting and emplacement

- mechanisms: *South Africa Journal of Geology*, v. 13, no. 4, p. 401–412.
- Harrison, T.N., 1988, Magmatic garnets in the Cairngorm granite, Scotland: *Mineralogical Magazine*, v. 52, p. 659–667.
- Hawkesworth, C.J., Blake, S., Evans, P., Hughes, R., Macdonald, R., Thomas, L.E., Turner, S.P., and Zellmer, G., 2000, Time scales of crystal fractionation on magma chambers-integrating physical, isotopic and geochemical perspectives: *Journal of Petrology*, v. 41, p. 991–1006.
- Heuss-Aßbichler, S., and Fehr, K.T., 1997, Intercrystalline exchange of Al and Fe<sup>3+</sup> between grossular-andradite and clinzoisite-epidote solid solutions: *Neues Jahrbuch für Mineralogie-Abhandlungen*, v. 172, p. 69–100.
- Hogan, J.P., 1996, Insights from igneous reaction space: a holistic approach to granite crystallization: *Earth and Environmental Science Transactions*, v. 87, p. 147–157.
- Holdaway, M.J., 2000, Application of new experimental and garnet Margules data to the garnet-biotite geothermometer: *American Mineralogist*, v. 85, p. 881–892.
- Holdaway, M.J., Mukhopadhyay, B., Dyar, M.D., Guidotti, C.V., and Dutrow, B.L., 1997, Garnet-biotite geothermometry revised; New Margules parameters and a natural specimen data set from Maine: *American Mineralogist*, v. 82, p. 582–595.
- Holland, T.J.B., and Blundy, J., 1994, Non-ideal interactions in calcic amphiboles and their bearing on amphibole-plagioclase thermometry: *Contributions to Mineralogy and Petrology*, v. 116, p. 433–447.
- Hollister, L.S., Grissom, G.C., Peters E.K., Stowell H., and Sisson V.B., 1987, Confirmation of the empirical correlation of Al in hornblende with pressure of solidification of calc-alkaline plutons: *American Mineralogist*, v. 72, p. 231–239.
- Johnson, M.C., and Rutherford, M.J., 1989, Experimental calibration of the aluminum-in-hornblende geobarometer with application to Long Valley Caldera (California) volcanic rocks: *Geology*, v. 17, no. 9, p. 837–841.
- Jung, S., Mezger, K., and Hoernes, S., 2001, Trace element and isotopic (Sr, Nd, Pb, O) arguments for a mid-crustal origin of Pan-African garnet-bearing S-type granites from the Damara orogen (Namibia): *Precambrian Research*, v. 110, p. 325–355.
- Kano, H., 1983, On the origin of garnets in the Setouchi andesites: *Scientific and Technical Report of Mining College, Akita University*, v. 4, p. 41–46.
- Kano, H., and Yashima, R., 1976, Almandine-garnets of acid magmatic origin from Yamanogawa, Fukushima prefecture and Kamitazawa, Yamagata prefecture: *The Japanese Association of Mineralogists, Petrologists and Economic Geologists*, v. 71, p. 106–119.
- Karimpour, M.H., Stern, C.R., and Farmer, L., 2010, Zircon U-Pb geochronology, Sr-Nd isotope analyses, and petrogenetic study of the Dehnow diorite and Kuhsangi granodiorite (Paleo-Tethys), NE Iran: *Journal of Asian Earth Sciences*, v. 37, p. 384–393.
- Kawabata, H., and Shuto, K., 2005, Magma mixing recorded in intermediate rocks associated with high-Mg andesites from the Setouchi volcanic belt, Japan: Implications for Archean TTG formation: *Journal of Volcanology and Geothermal Research*, v. 140, no. 4, p. 241–271.
- Kawabata, H., and Takafuji, N., 2005, Origin of garnet crystals in calc-alkaline volcanic rocks from the Setouchi volcanic belt, Japan: *Mineralogical Magazine*, v. 69, p. 951–971.
- King, E.M., and Valley, J.W., 2001, The source, magmatic contamination, and alteration of the Idaho Batholith: *Contributions to Mineralogy and Petrology*, v. 142, p. 72–88.
- Kohn, M.J., Spear, F.S., and Valley, J.W., 1997, Dehydration melting and fluid recycling during metamorphism: Rangeley Formation, New Hampshire, USA: *Journal of Petrology*, v. 38, p. 1255–1277.
- Konrad-Schmalke, M., Handy, M.R., Babist, J., and O'Brien, P. J., 2005, Thermodynamic modeling of diffusion-controlled garnet growth: *Contributions to Mineralogy and Petrology*, v. 16, p. 181–195.
- Korolyuk, V.N., and Lepegin, G.G., 2008, Analysis of experimental data on the diffusion coefficients of Fe, Mn, Mg, and Ca in garnets: *Russian Geology and Geophysics*, v. 49, p. 557–569.
- Kretz, R., 1983, Symbols for rock forming minerals: *American Mineralogist*, v. 68, no. 1/2, p. 277–279.
- Lackey, J.S., Romero, G.A., Bouvier, A.S., and Valley, J.W., 2012, Dynamic growth of garnet in granitic magmas: *Geology*, v. 40, p. 171–174.
- Lackey, J.S., Valley, J.W., Chen, J.H., and Stockli, D.F., 2008, Dynamic magma systems, crustal recycling, and alteration in the Central Sierra Nevada Batholith: The oxygen isotope record: *Journal of Petrology*, v. 49, no. 7, p. 1397–1426.
- Lackey, J.S., Valley, J.W., and Hinke, H.J., 2006, Deciphering the source and contamination history of peraluminous magmas using δ<sup>18</sup>O of accessory minerals: Examples from garnet-bearing plutons of the Sierra Nevada batholiths: *Contributions to Mineralogy and Petrology*, v. 151, p. 20–44.
- Leake, B.E., Alan, R.W., William, D.B., Ernst, A.J.B., Giovanni, F., Jeol, D.J., Frank, C.H., Hanan, J.K., Vladimir, G.K., John, C.S., Nicholas, C.N.S., and Eric, J.W.W., 2004, Nomenclature of amphiboles: Additions and revisions to the International Mineralogical Associations amphibole nomenclature: *American Mineralogist*, v. 89, p. 883–887.
- Lyons, J.B., and Morse, S.A., 1970, Mg/Fe partitioning in garnet and biotite from some granitic, pelitic, and calcic rocks: *American Mineralogist*, v. 55, p. 231–245.
- Manning, D.A.C., 1983, Chemical variation in garnets from aplites and pegmatites, peninsular Thailand: *Mineralogical Magazine*, v. 47, p. 353–358.
- Mason, P.R.D., Downes, H., Thirlwall, M., Seghedi, I., Szakacs, A., Lowry, D., and Matthey, D., 1996, Crustal assimilation as a major petrogenetic process in east Carpathian Neogene to Quaternary continental margin arc magmas: *Journal of Petrology*, v. 37, p. 927–959.
- Miller, C.F., and Stoddard, E.F., 1981, The role of manganese in the paragenesis of magmatic garnet: An example from the Old Woman-Plute Range, California: *Journal of Geology*, v. 89, p. 233–246.
- Mirnejad, H., Blourian, G.H., Kheirkhah, M., Akrami, M.A., and Tutti, F., 2008, Garnet-bearing rhyolite from Deh-Salm area, Lut block, Eastern Iran: Anatexis of deep crustal rocks: *Mineralogy and Petrology*, v. 94, no. 3–4, p. 259–269.
- Mirnejad, H., Lalonde, A.E., Obeid, M., and Hassanzadeh, J., 2013, Geochemistry and petrogenesis of Mashhad granitoids: An insight into the geodynamic history of the Paleo-Tethys in Northeast of Iran: *Lithos*, v. 170–171, p. 105–116.
- Moazez-Lesco, Z., and Plimer, I.R., 1979, Intrusive and poly-metamorphic rocks of the Darakht-Bid Area, near Mashhad, Iran: *Geologische Rundschau*, v. 68, no. 1, p. 318–383.
- Nabavi, M., 1976, An introduction to the geology of Iran: Tehran, Geological Survey of Iran, 109 p.
- Natalin, B.A., and Sengör, A.M.C., 2005, Late Paleozoic to Triassic evolution of the Turan and Scythian platforms: The pre-history of the Palaeo-Tethyan closure: *Tectonophysics*, v. 404, p. 175–202.

- Öztürk, Y.Y., Helvaci, C., and Satir, M., 2012, Geochemical and isotopic constraints on petrogenesis of the Beypazarı Granitoid, NW Ankara, Western Central Anatolia, Turkey: Turkish Journal of Earth Sciences, v. 21, p. 53–77.
- Patranabis-Deb, A., Schieber, J., and Basu, A., 2009, Almandine garnet phenocrysts in a 1Ga rhyolitic tuff from Central India: Geological Magazine, v. 146, no. 1, p. 133–143.
- Plank, T., 1987, Magmatic garnets from the Cardigan pluton and the Acadian thermal event in southwest New Hampshire: American Mineralogist, v. 72, p. 681–688.
- Plimer, I.R., and Moazez-Lesco, Z., 1981, Polymetamorphic normal, reverse zoned and unzoned garnets from the Darakht-Bid aureole, Mashhad, Iran: Mineralogy and Petrology, v. 28, p. 245–263.
- Poli, S., and Schmidt, M.W., 2004, Experimental subsolidus studies on epidote minerals: Reviews in Mineralogy and Geochemistry, v. 56, p. 171–195.
- Rene, M., and Stelling, J., 2007, Garnet-bearing granite from the Trebic pluton, Bohemian Massif (Czech Republic): Mineralogy and Petrology, v. 91, p. 55–69.
- Samadi, R., 2009, The origin of garnet megacrysts from Dehnow Tonalite, Northwest of Mashhad [M.Sc. Thesis in Petrology]: Tehran, Iran, University of Tehran, 179 p.
- Samadi, R., Mirnejad, H., Shirdashtzadeh, N., and Kawabata, H., 2012a, Application of garnet chemistry in thermodynamic studies of Dehnow Tonalite (Northwest of Mashhad): Iranian Journal of Crystallography and Mineralogy, v. 20, no. 2, p. 253–264.
- Samadi, R., Valizadeh, M.V., Mirnejad, H., and Kawabata, H., 2012b, Geothermometry and geobarometry of metamorphic rocks of Dehnow (Northwest of Mashhad): Journal of Geosciences, v. 21, no. 84, p. 3–14.
- Samadi, R., Gazel, E., Mirnejad, H., Kawabata, H., A.A., Baharifar, and S.J. Sheikh Zakariaee, 2014, Triassic Paleo-Tethys subduction in the center of the Alpine-Himalayan Orogen: Evidence from Dehnow I-type granitoids (NE Iran): Neues Jahrbuch für Geologie und Paläontologie, v. 271/3 (in press). DOI: 10.1127/0077-7749/2014/0390.
- Scallion, K.L., Jamieson, R.A., Barr, S.M., White, C.E., and Erdmann, S., 2011, Texture and composition of garnet as a guide to contamination of granitoid plutons: An example from the Governor Lake area, Meguma Terrane, Nova Scotia: The Canadian Mineralogist, v. 49, no. 2, p. 441–458.
- Scheibner, B., Werner, G., Civetta, L., Stosch, H.G., Simon, K., and Kronz, A., 2007, Rare earth element fractionation in magmatic Ca-rich garnets: Contributions to Mineralogy and Petrology, v. 154, p. 55–74.
- Schmidt, M.W., 1992, Amphibole composition in tonalite as a function of pressure: An experimental calibration of the Al-in-hornblende barometer: Contributions to Mineralogy and Petrology, v. 110, p. 304–310.
- Sharp, Z.D., 2006, Principles of stable isotope geochemistry: Upper Saddle River, NJ, Pearson Education, 344 p.
- Spear, F.S., 1993, Metamorphic Phase Equilibria and Pressure-Temperature-Time Paths: Monograph, Mineralogical Society of America, Washington, 799 p.
- Spear, F.S., and Cheney, J.T., 1989, A petrogenetic grid for pelitic schists in the system  $\text{SiO}_2\text{-Al}_2\text{O}_3\text{-FeO}\text{-MgO}\text{-K}_2\text{O}$ - $\text{H}_2\text{O}$ : Contributions to Mineralogy and Petrology, v. 101, p. 149–164.
- Taylor, H.P., Jr., and Sheppard, S.M.F., 1986, Igneous rocks: I. Processes of isotopic fractionation and isotope systematics, in Valley, J.W., Taylor, H.P., Jr., and O'Neil, J.R., eds., Stable isotopes in high temperatures geological processes: Review in Mineralogy, Washington, DC, Mineralogical Society of America, v. 16, p. 227–271.
- Taylor, J., and Stevens, G., 2010, Selective entrainment of peritectic garnet into S-type granitic magmas: Evidence from Archaean mid-crustal anatectites: Lithos, v. 120, p. 277–292.
- Tuccillo, M.E., Essene, E.J., and van der Pluijm, B.A., 1990, Growth and retrograde zoning in garnets from high-grade metapelites: Implications for pressure-temperature paths: Geology, v. 18, p. 839–842.
- Valley, J.W., Bindeman, I.N., and Peck, W.H., 2003, Empirical calibration of oxygen isotope fractionations in zircon: Geochimica et Cosmochimica Acta, v. 67, no. 17, p. 3257–3266.
- Vennum, W.R., and Meyer, C.E., 1979, Plutonic garnets from the Werner batholith, Lassiter Coast, Antarctic Peninsula: American Mineralogist, v. 64, p. 268–273.
- Vielzeuf, D., and Montel, J.M., 1994, Partial melting of meta-greywackes, Part I. Fluid-absent experiments and phase relationships: Contributions to Mineralogy and Petrology, v. 117, p. 375–393.
- Vielzeuf, D., Veschambre, M., and Brunet, F., 2005, Oxygen isotope heterogeneities and diffusion profile in composite metamorphic-magmatic garnets from the Pyrenees: American Mineralogist, v. 90, p. 463–472.
- Villaro, A., Stevens, G., and Buick, I.S., 2009, Tracking S-type granite from source to emplacement: Clues from garnet in the Cape Granite Suite: Lithos, v. 112, p. 217–235.
- Whitney, D.L., and Evans, B.W., 2010, Abbreviations for names of rock-forming minerals: American Mineralogist, v. 95, p. 185–187.
- Wu, C.M., Zhang, J., and Ren, L.D., 2004, Empirical garnet-biotite-plagioclase-quartz (GBPQ) geobarometry in medium to high grade metapelites: Journal of Petrology, v. 45, p. 1907–1921.
- Yuan, C., Sun, M., Xiao, W., Wilde, S., Li, X., Liu, X., Long, X., Xia, X., Ye, K., and Li, J., 2008, Garnet-bearing tonalitic porphyry from East Kunlun, Northeast Tibetan Plateau: implications for adakite and magmas from the MASH Zone: International Journal of Earth Science (Geologische Rundschau), v. 98, no. 6, p. 1489–1510.
- Zhang, J., Ma, C., and She, Z., 2012, An Early Cretaceous garnet-bearing metaluminous A-type granite intrusion in the East Qinling Orogen, Central China: Petrological, mineralogical and geochemical constraints: Geoscience Frontiers, v. 3, no. 5, p. 635–646.
- Zhang, L., Zhong, Z., Zhang, H., Sun, W., and Xiang, H., 2009, The formation of foliated (garnet-bearing) granites in the Tongbai-Dabie orogenic belt: partial melting of subducted continental crust during exhumation: Journal of Metamorphic Geology, v. 27, p. 789–803.
- Zheng, Y.F., 1993, Calculation of oxygen isotope fractionation in anhydrous silicate minerals: Geochim Cosmochim Acta, v. 57, p. 1079–1091.